DTU Library

Characterization of the genetic switch from phage φ13 important for Staphylococcus aureus colonization in humans

Kristensen, Camilla S.; Varming, Anders K.; Leinweber, Helena A. K.; Hammer, Karin; Lo Leggio, Leila; Ingmer, Hanne; Kilstrup, Mogens

Link back to DTU Orbit

ORIGINAL ARTICLE

MicrobiologyOpen WILEY

Characterization of the genetic switch from phage φ13 important for *Staphylococcus aureus* colonization in humans

Camilla S. Kristensen[1] | Anders K. Varming[2] | Helena A. K. Leinweber[3] | Karin Hammer[1] | Leila Lo Leggio[2] | Hanne Ingmer[3] | Mogens Kilstrup[1]

[1]Department of Biotechnology and Biomedicine, Technical University of Denmark, Lyngby, Denmark

[2]Department of Chemistry, University of Copenhagen, Kobenhavn, Denmark

[3]Department of Veterinary and Animal Sciences, University of Copenhagen, Kobenhavn, Denmark

Correspondence
Mogens Kilstrup, Department of Biotechnology and Biomedicine, Technical University of Denmark, Denmark.
Email: mki@bio.dtu.dk

Abstract

Temperate phages are bacterial viruses that after infection either reside integrated into a bacterial genome as prophages forming lysogens or multiply in a lytic lifecycle. The decision between lifestyles is determined by a switch involving a phage-encoded repressor, CI, and a promoter region from which lytic and lysogenic genes are divergently transcribed. Here, we investigate the switch of phage φ13 from the human pathogen *Staphylococcus aureus*. φ13 encodes several virulence factors and is prevalent in *S. aureus* strains colonizing humans. We show that the φ13 switch harbors a *cI* gene, a predicted *mor* (modulator of repression) gene, and three high-affinity operator sites binding CI. To quantify the decision between lytic and lysogenic lifestyle, we introduced reporter plasmids that carry the 1.3 kb switch region from φ13 with the lytic promoter fused to *lacZ* into *S. aureus* and *Bacillus subtilis*. Analysis of β-galactosidase expression indicated that decision frequency is independent of host factors. The white "lysogenic" phenotype, which relies on the expression of *cI*, could be switched to a stable blue "lytic" phenotype by DNA damaging agents. We have characterized lifestyle decisions of phage φ13, and our approach may be applied to other temperate phages encoding virulence factors in *S. aureus*.

KEYWORDS
bacteriophage, genetic switch, lysogeny, φ13, phi13, prophage, repressor, *Staphylococcus aureus*

1 | INTRODUCTION

Staphylococcus aureus is a Gram-positive, opportunistic human pathogen causing millions of infections worldwide each year, ranging from skin and soft tissue infections, food poisoning, endocarditis, and respiratory tract infections to bacteremia, amongst many others (Liu, 2009; Lowy, 1998; Tong et al., 2015). The severity of the infections varies from mild to life-threatening, largely determined by the various virulence factors contained in the infecting strain.

A number of important virulence factors are encoded by *S. aureus* prophages that stably reside in the bacterial genome (Xia & Wolz, 2014). Most clinical strains of *S. aureus* are lysogens and carry between one and four prophages that encode important toxins, such as Panton-Valentine leucocidin (PVL) and enterotoxins (Ingmer et al., 2019). Some of the most common prophages in human isolates of *S. aureus* belong to the Sa3int group. These phages integrate into the *hlb* gene of *S. aureus* and express an immune evasion cluster encoding several virulence factors promoting colonization (Coleman et al.,

1991; Xia & Wolz, 2014). As the beta-hemolysin encoded by _hlb_ is also a virulence factor (Huseby et al., 2007; Katayama et al., 2013), this negative conversion appears counterintuitive, but Sa3int phages have been shown to excise and remain as pseudo-lysogens, allowing expression of both the beta-hemolysin and the virulence factors encoded by the phage (Goerke et al., 2006; Katayama et al., 2013; Salgado-Pabón et al., 2014).

Temperate phages have a dual lifecycle involving either lytic replication and production of active phages or being inserted in and replicated with the bacterial chromosome. The decision between these lifestyles is made by a phage-encoded (epi)genetic switch. Phage λ, targeting _Escherichia coli_, offers the classical example of such a switch, where a complex decision phase determines from which of the two involved promoters, P_R or P_{RM}, transcription occurs. Expression from the P_{RM} promoter produces the phage repressor CI, whereas expression from P_R allows the production of the Cro repressor, as well as other gene products needed for producing active phage particles (Casjens & Hendrix, 2015; Oppenheim et al., 2005). Stable expression from the P_{RM} promoter is needed for the maintenance of the λ chromosome into the _E. coli_ chromosome. It also produces a high concentration of the CI repressor, which is required for activation of the P_{RM} promoter and tight repression of the P_R promoter in the integrated prophage and any incoming λ phages, rendering the lysogenic bacterium immune to secondary attacks. The decision and integration of phage λ are not solely dependent upon the phage-encoded factors, as _E. coli_ host factors also affect this process (Grodzicker et al., 1972; Herman et al., 1993; Kihara et al., 2001; Roucourt & Lavigne, 2009). The escape of phage λ from the lysogenic state can be initiated by autocleavage of the CI repressor. In a process analogous to autocleavage of the LexA repressor, CI is bound to activated RecA filaments polymerized on single-stranded DNA during the SOS DNA damage response, leading to activation of CI auto-peptidase activity (Atsumi & Little, 2006; Little, 1984; Oppenheim et al., 2005). A quite different switch mechanism is used by the TP901-1 phage infecting the Gram-positive bacterium _Lactococcus lactis_ (Madsen et al., 1999) which shares extensive homology to the φ13 switch (Pedersen et al., 2020). Here, a CI repressor, expressed from the lysogenic promoter P_R, represses the lytic P_L promoter. A small repressor (MOR, for modulator of repression) expressed from the P_L promoter represses the P_R promoter; however, it does require CI as a co-repressor. In addition MOR functions as an antirepressor against CI (Pedersen & Hammer, 2008).

As a member of the staphylococcal Sa3int phage family, the bacteriophage φ13 shares features with the other members. These features include the Sa3 type integrase and the presence of the _sak_, _chp_, and _scn_ virulence genes (Goerke et al., 2009; Xia & Wolz, 2014), but an analysis of the genetic switches within the group has never been reported.

To characterize the switch from phage φ13, we have compared its switch region to the switch regions in TP901-1 and the switch regions in _Staphylococcus_ phages, showing that a group of phages with the Sa3 integrase shares similar switch regions containing CI and MOR homologs. We have purified the φ13 CI repressor and

shown that it interacts with three palindromic sites in the switch region. By constructing plasmids containing the φ13 genetic switch with _lacZ_ reporter fusions to the lytic promoter (switch plasmids) and analysis of the frequency of Lac phenotypes in transformants of the natural and a heterologous host, we have shown that a functional _mor_ gene is required for "decision switching" and that this process is independent of staphylococcal host factors. The concept of "toggle switching" has previously been defined as "the induced or accidental change from one stable phenotype to another from a bistable switch" (Gardner et al., 2000). Thus, toggle switching is when the phage changes its state, either spontaneously or following induction. In contrast, decision switching is when the phage initially establishes itself as lytic or lysogenic, in a process that precedes toggle switching. In the current study, φ13 switch plasmids were found to toggle spontaneously from the "lytic" (Lac+, blue) colony phenotype to a stable "lysogenic" (Lac−, white) colony phenotype. In the opposite direction, toggling from the stable "lysogenic" colony phenotype to the "lytic" colony phenotype could readily be induced by sub-lethal concentrations of DNA damaging agents. The results from this study can prove important in the analysis of _S. aureus_ virulence in vivo by determining conditions during infection that would result in induction and spread of φ13 and the unwanted establishment of φ13 prophages in susceptible hosts. The results may ultimately aid in the understanding of how some Sa3int prophages are disseminated in society and suggest ways to limit _S. aureus_ colonization in humans.

2 | EXPERIMENTAL PROCEDURES

2.1 | Growth specifications

Unless otherwise specified, _E. coli_ and _Bacillus subtilis_ were grown in lysogeny broth (LB) or LB agar, while _S. aureus_ was grown in tryptic soy broth (TSB) or agar (TSA). All strains were grown at 37°C with sufficient aeration and the addition of appropriate antibiotics. 5-Bromo-4-chloro-3-indolyl-β-D-galactopyranoside (X-gal) was added to agar plates at 100–200 μg ml^{-1}.

Phages were stored and diluted in SM buffer (100 mM NaCl, 8 mM MgSO$_4$·7H$_2$O, 50 mM Tris-CL (pH 7.5)).

2.2 | Bacterial strains and plasmids

All bacterial strains used in this study can be found in Table A1, while selected strains, plasmids, and phages are summarized in Tables 1–3, respectively.

2.3 | Protein expression and purification

A synthetic codon-optimized gene for recombinant CI repressor protein with an N-terminal His-tag and TEV cleavage site (φ13 rCI) was purchased from Genscript (Figure A1) in a pET30a(+) expression

TABLE 1 List of selected bacterial strains used in this study

Strain	Species	Short description or relevant genotype	Reference or source
168	*B. subtilis*		Burkholder and Giles (1947)
8325-4	*S. aureus*	NCTC8325 phage cured	Novick (1967)
8325-4 φ13-kana	*S. aureus*	8325-4 lysogenized with φ13-kana	Tang et al. (2017)
CSK8	*B. subtilis*	168 *thrC*::pCSK2 expressing the "lytic" phenotype	This study
CSK9	*B. subtilis*	168 *thrC*::pCSK2 expressing the "lysogenic" phenotype	This study
CSK10	*B. subtilis*	168/pCSK3 expressing the "lytic" phenotype	This study
CSK11	*B. subtilis*	168/pCSK3 expressing the "lysogenic" phenotype	This study
CSK32	*S. aureus*	8325-4/pCSK3 expressing the "lytic" phenotype	This study
CSK33	*S. aureus*	8325-4/pCSK3 expressing the "lysogenic" phenotype	This study
CSK47	*S. aureus*	CSK45 *geh*::pCSK9 expressing the "lytic" phenotype	This study
CSK48	*S. aureus*	CSK45 *geh*::pCSK9 expressing the "lysogenic" phenotype	This study
CSK56	*S. aureus*	CSK46 *geh*::pCL25	This study
CSK59	*S. aureus*	8325-4/pNZlac	This study
CSK68	*S. aureus*	CSK45 *geh*::pCL25	This study

Note: Strain, species, a short description, and reference of selected strains. See Table A1 for a complete list.

vector. The expression vector was transformed into BL21 (DE3) *E. coli* cells and grown at 37°C. φ13 rCI expression was induced by 0.5 mM isopropyl β-D-1-thiogalactopyranoside in a mid-exponential culture and the temperature lowered to 25°C.

After 20 h, cells were harvested and sonicated. The cell lysate was collected and filtered through a 0.22 μm filter. Chromatographic purification was done on an ÄKTA purifier 10 system (GE Healthcare Life Sciences) by immobilized metal affinity chromatography (IMAC; HisTrap HP 1 ml column) and size exclusion chromatography (SEC; HiLoad 26/600 Superdex200 column). 20 mM Tris, 20 mM imidazole, 1 M NaCl, pH 8.0 was used as washing buffer and 20 mM Tris, 500 mM imidazole, 100 mM NaCl, pH 8.0 as elution buffer in IMAC, while 20 mM Tris, 100 mM NaCl, pH 7.5 was used as SEC buffer. Blue Dextran (2000 kDa), Ferritin (440 kDa), Catalase (232 kDa), Aldolase (158 kDa), Carbonic Anhydrase (29 kDa), and Aprotinin (6.5 kDa) were used as Mw standards in SEC.

Protein purity was assessed by SDS-PAGE (15% gels).

The protein concentration was estimated by A_{280} using an extinction coefficient of 26 360 M^{-1} cm^{-1} (tagged) and 23 380 M^{-1} cm^{-1} (untagged) as estimated with ProtParam (http://web.expasy.org/protparam) (Gasteiger et al., 2005).

For EMSA using native CI, the tag on φ13 rCI was removed beforehand by mixing the protein 10:1 with TEV protease (Sigma Aldrich) and incubating it at 4°C for 3 days. The uncleaved protein was separated from the mixture by IMAC and the flowthrough was collected for use.

2.4 | DSF and CD spectroscopy

The inflection temperature, T_i, was determined using a Nanotemper Tycho™ NT.6 DSF monitoring changes in the ratio of intrinsic fluorescence at 350 and 330 nm while heating from 35°C to 95°C with a temperature ramp of 30°C min^{-1}. The sample was loaded in high precision glass capillaries with a concentration of 4.9 μM.

For CD spectroscopy, the purified protein was transferred to a 20 mM NaF buffer, pH 7.5. The experiments were conducted on a Jasco J-815 CD spectropolarimeter in a suprasil quartz cell with a 1 mm light path (Hellma Analytics) and a sample concentration of 1.56 μM. The spectra were measured at room temperature in a continuous mode at 20 nm min^{-1} from 260 to 190 nm with a data pitch and bandwidth of 1 nm, averaging five spectra per measurement and subtracting the buffer spectra. The CD spectrum was deconvoluted and analyzed using DichroWeb (Whitmore & Wallace, 2008) with the CDSSTR method (Sreerama & Woody, 2000) and reference sets 3 and 6 and by BeStSel (Micsonai et al., 2015, 2018).

Plasmid	Description	Reference or source
pDG1729	Promoterless LacZ reporter plasmid integrating in _B. subtilis_ in _thrC_	Guérout-Fleury et al. (1996)
pNZlac	Promoterless replicative LacZ reporter plasmid	Kovács et al. (2010)
pCSK2	φ13 switch inserted in pDG1729, _lacZ_ fused to P_L downstream of _mor_	This study
pCSK3	φ13 switch inserted in pNZlac, _lacZ_ fused to P_L downstream of _mor_	This study
pCL25	Promoterless integration plasmid integrating into $attB^{L54a}$ in _geh_ of _S. aureus_	Luong and Lee (2007)
pYL112Δ19	Contains L54a integrase. Needed for integration of pCL25 derivatives in _S. aureus_	Lee et al. (1991)
pCSK9	φ13 switch and _lacZ_ of pCSK2 inserted in pCL25	This study
pCSK11	As pCSK2, with disrupted _mor_ start codon (ATG to ATC)	This study
pCSK12	As pCSK9, with disrupted _mor_ start codon (ATG to ATC)	This study
pCSK13	As pCSK3, with disrupted _mor_ start codon (ATG to ATC)	This study
pET30a(+)	Expression vector containing φ13 rCI gene	This study

Note: Plasmid name, a short description, and reference included for all plasmids.

Phage	Description	Reference
φ13-kana	Fully functional φ13 containing a kanamycin resistance cassette	Tang et al. (2017)
φ11	Generally transducing _S. aureus_ phage	Novick (1967)
φ80α	Generally transducing _S. aureus_ phage	Novick (1963)
SPP1	Generally transducing _B. subtilis_ phage	Riva et al. (1968)

Note: Phages used, a brief description of these, and a reference of origin included.

2.5 | Synthesis and labeling of DNA fragments

For gel shift assays, DNA fragments containing each of the three operator sites, O_R, O_L, and O_D, were synthesized by PCR with appropriate annealing temperatures using a Phusion polymerase. Non-fluorescent probes were created by amplifying the genetic switch region of φ13 with primers MK867 and MK868 for O_R, MK869 and MK870 for O_L, and MK871 and MK872 for O_D. The DNA fragments were made fluorescent by a second PCR run with the Cy5-containing primers MK740 and MK741. Mutated probes with altered operator half-sites (TTCA to TTGA) were amplified from the non-fluorescent probes in two steps. First overlapping left and right half parts were amplified: O_R left part from the O_R probe using MK1038 and MK741; O_R right part from the O_R probe using MK1039 and MK740; O_L left part from the O_L probe using MK1040 and MK741; O_L right part from the O_L probe using MK1041 and MK740; O_D left part from the O_D probe using MK1042 and MK741; O_D right part from the O_D probe using MK1043 and MK740. Full-length mutant probes were synthesized with the overlapping left parts and right parts as templates and mega-primers in a subsequent PCR reaction, followed by amplification of the product with fluorescent primers MK740 and MK741. See Table A2 for a list of primers used in this study.

2.6 | EMSA

Tagged and detagged φ13 rCI was mixed with binding buffer (100 mM Tris-HCl, 5 mM EDTA, 500 mM NaCl, 5 mM DTT, 25% glycerol), bovine serum albumin, and sheared DNA. In each assay, ~0.5 nM DNA probe was mixed with varying concentrations of rCI in a total of 20 μl binding solution. After pre-incubation on ice for 15 min, the DNA fragment was added and incubation was continued for 30 min. The mixture was then transferred into the empty wells of a chilled 2% agarose gel and run horizontally in 1× TBE (Tris/Borate/EDTA) buffer for 90 min at a constant voltage of 110 at 0°C. For visualization and quantification, the gel was scanned directly in a STORM 860 Imager (Amersham Biosciences) using the red channel (635 nm) at high sensitivity, followed by image editing using the ImageQuant

TL software (Amersham Biosciences). The image was analyzed using Fiji (Schindelin et al., 2012). The integrated density of each band was measured and used to calculate the individual fractions of protein bound to DNA at each protein concentration. The data were fitted using the non-linear curve fitting option and the specific binding with Hill slope option in GraphPad Prism (GraphPad Software, Inc.).

2.7 | Construction of switch plasmids

All PCRs were conducted at appropriate annealing temperature and elongation time using Phusion polymerase unless otherwise specified. All switch plasmids contained the entire genetic switch of φ13 with a *lacZ* gene translationally fused to P$_L$ downstream of *mor*, and all constructs were verified by sequencing. pCSK2 was created by amplifying the genetic switch region of φ13 from 8325-4 φ13 with primers MK860 and MK863, digestion by EcoRI and BamHI, followed by ligation into digested pDG1729. From pCSK2, the switch region and *lacZ* gene were amplified by primers MK863 and MK902, digested by EcoRI and BglII, and ligated into pCL25 digested by EcoRI and BamHI creating pCSK9. pCSK3 was constructed by amplifying the switch region of φ13 from 8325-4 φ13 with primers MK861 and MK862, digestion by XbaI and SphI, followed by ligation into digested pNZlac. The start codon of *mor* was mutated (ATG to ATC) in pCSK2, pCSK3, and pCSK9 by use of CloneAmp™ HiFi PCR Premix Polymerase resulting in pCSK11, pCSK13, and pCSK12. The primers MK914 and MK915 were used to amplify the entire plasmid while incorporating the point mutation.

2.8 | Transformations

Electrocompetent *E. coli* cells were created and electroporated as previously described (Pedersen et al., 2020). Cells were plated on selective agar plates after 1 h of recovery.

Competent *B. subtilis* cells were obtained as described in (Konkol et al., 2013) with one minor change; 30 min after plasmid addition equal volumes of LB media were added to the transformation mixture, followed by incubation for 1 h and plating on selective plates.

Transformations in *S. aureus* were performed using the procedure for electroporation described in (Monk et al., 2015). pYL112Δ19 was transformed into 8325-4 and 8325-4 φ13-kana before the introduction of integrating plasmids to supply the required integrase.

2.9 | Transductions

Transductions in *B. subtilis* and *S. aureus* were accomplished by using phage SPP1 or φ11/φ80α, respectively. See Table 3 for all phages used in this study. Transducing phage stocks were prepared as plate lysates on the donor strains by allowing phage adsorption for 15 min at 37°C with 5 mM CaCl$_2$ and subsequent plating in top agar (LB/TSB, 0.5% agar, 5 mM CaCl$_2$). After overnight incubation, the top

layer was suspended in SM, centrifuged at 5000 *g* for 10 min, and the supernatant was filter-sterilized (0.2 μm). Transducing phages were added at a multiplicity of infection (MOI) of 10 to *B. subtilis* 168 and MOI = 0.1 to *S. aureus* 8325-4 and 8325-4 φ13, followed by 15 min incubation at 37°C. Cells were washed with equal volumes of 20 mM Na-citrate and plated on selective plates containing X-gal and 20 mM Na-Citrate.

2.10 | Stability of switch plasmid phenotypes

To examine the stability of the "lysogenic" and "lytic" phenotype of the switch plasmids, a single colony resulting from transformation was suspended in an appropriate medium, diluted, and plated at a density allowing the formation of single colonies for phenotype determination.

2.11 | Plate inductions

To test the effect of inducing substances, both *B. subtilis* and *S. aureus* cells containing switch plasmids were plated at a cell density resulting in around 1000 colonies per plate, obtained by suspending a colony in LB/TSA medium, dilutions, and plating; 3 μl inducing substance (0.5 mg ml^{-1} mitomycin C, 1 mg ml^{-1} ciprofloxacin, or 30% hydrogen peroxide) was applied to the middle of the plate, followed by incubation at 37°C. When relevant, selected colonies were suspended in media, diluted, and plated at a density resulting in single colonies to determine phenotypes.

2.12 | Temporal induction

A culture of 8325-4 *geh*::pCSK9 favoring the "lysogenic" phenotype (CSK48) was inoculated in TSB and grown to OD$_{600}$ = 0.6 followed by induction by 1 μg ml^{-1} mitomycin C. Samples were taken periodically, diluted in TSB, and plated on selective TSA plates containing X-gal. Switch plasmid phenotypes were determined after overnight incubation.

2.13 | Phage infection of 8325-4 harboring switch plasmids

Cultures were inoculated in TSB and grown to OD$_{600}$ = 0.6. At this point, a sample was plated for determination of colony forming units (CFU) ml^{-1}, after which, phages were added at a MOI of 0.1, followed by incubation for 2 h. Cultures were spun at 5000 *g* for 5 min and the supernatant filter-sterilized (0.2 μm), followed by dilution in SM buffer, titration on bacterial lawns of 8325-4 (TSB, 0.5% agarose, 5 mM CaCl$_2$), and overnight incubation for determination of plaque forming units (PFU) ml^{-1}. The amount of phages produced per host cell was determined by calculating PFU ml^{-1} per CFU ml^{-1}.

2.14 | Lysogenization frequency of φ13

Exponential cultures of 8435-4 were infected with φ13-kana at a MOI of 0.1 and 1. Phages were allowed to adsorb for 15 min on ice, after which cells were centrifuged and the pellet was resuspended in SM buffer. Dilutions were plated on TSA plates containing kanamycin for the determination of lysogens. Dilutions were further titrated on bacterial lawns of 8435-4 to detect cells in which the phage favored the lytic lifecycle. Phage titer was determined as PFU ml^{-1} after overnight incubation. The lysogenization frequency was calculated as the ratio of lysogenic cells (CFU (Kan^R) ml^{-1}) of all infected cells (CFU (Kan^R) ml^{-1} + PFU ml^{-1}).

3 | RESULTS AND DISCUSSION

3.1 | Topology of the φ13 switch region and detection of identical switches in members of the Sa3int and the PVL encoding phages

Recently, a global search for DNA sequences similar to the phage TP901-1 switch region led us to identify a putative switch region in the *S. aureus* phage φ13 (Pedersen et al., 2020). As shown in the map in Figure 1 and the amino acid sequence alignments in Figure A2, the homology spans the N-terminal part of the *cl* gene, the intergenic region, and a divergently oriented, putative *mor* gene. Putative P_L and P_R promoters and O_R, O_L, and O_D operators were recognized in the φ13 switch in similar locations as in TP901-1 (Pedersen et al., 2020). The limited similarity was found to the C-terminal domain CI-CTD$_1$ from TP901-1, whereas the CI-CTD$_2$ showed no sign of conservation (Figure A2). Instead of the CI-CTD$_2$ domain, the CI repressor from φ13 carries a region with clear similarity to the C-terminal domain of the CI repressor from phage λ (see Figure A2). The two catalytic

residues from the peptidase domain as well as the autocatalytic site from λ are conserved in φ13, suggesting that the CI repressor from φ13, in contrast to the CI repressor from TP901-1 (Madsen et al., 1999), could be capable of autocleavage.

To analyze if the φ13 switch type was widespread among phages, we performed a homology search (Altschul et al., 1990) with the 1260 bp φ13 DNA sequence covering the region shown in Figure 1, excluding staphylococcal genome sequences. Only sequences from completed genomes of staphylococcal phages were identified, and six phages had hits with full coverage and sequence identity (>99% identity): PVL, tp301-1, P630, 3AJ-2017, IME1346_01, and φ13. Two of these, 3AJ-2017 and IME1346_01, encode the virulence proteins Sac, Chp, and Scn (Oliveira et al., 2019) and belong to the Sa3int group like φ13, while the phages PVL and tp301-1 encoded the LukS-PV and LukF-PV PVL virulence factors (Oliveira et al., 2019). This shows that the homology between the switches from φ13 and TP901-1 is not unique and that the φ13 switch type determines the decisions between lysogenic and lytic growth for two important groups of phages carrying pathogenicity genes.

3.2 | φ13 CI binds to operator sites in the intergenic region between *cl* and *mor*

To characterize the switch present in φ13, it was first important to know that the postulated CI repressor was functional and had an affinity towards the postulated CI operators. To determine whether the CI repressor from φ13 binds to these putative operators, CI was expressed with an N-terminal His-TEV-tag (termed rCI, see Figure A1) and purified by affinity chromatography and gel filtration (Figure A3a,b). After circular dichroism spectroscopy and differential scanning fluorimetry had confirmed that the protein was folded and stable (Figure A3c,d), electrophoretic mobility shift assays (EMSA) were
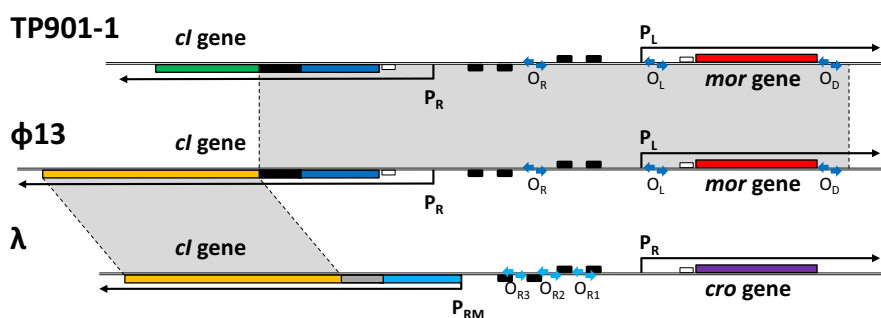
FIGURE 1 Comparison of switch regions from *S. aureus* phage φ13, *L. lactis* phage TP901-1, and *E. coli* phage λ. The geometry of the switch region is not shown to scale. The *mor* gene of TP901-1 and φ13 is shown as a red box, the *cro* gene of λ is shown as a purple box, and the first part of the *cl* gene encoding the DNA binding N-terminal domain (CI-NTD) is shown as a blue box. The part of the *cl* gene from φ13 encoding the extreme C-terminal domain (CI-CTD$_2$) is not homologous to the CI-CTD$_2$ domain in TP901-1 but to the C-terminal domain from CI of λ, containing a peptidase domain. CI-CTD$_2$ is shown as a green box for TP901-1 and a yellow box for φ13 and λ. A dimerization domain (CI-CTD$_1$) with helical hook structures in TP901-1 connects CI-CTD$_2$ and CI-NTD and is shown as a black box for TP901-1 and φ13, while the dimerization region is shown as a gray box for λ. The divergently oriented promoters, P_R and P_L for TP901-1, P_{RM} and P_R for λ, and putative P_R and P_L promoters for φ13, are shown as arrows preceded by small black boxes symbolizing −10 and −35 regions. Small white boxes indicate ribosomal binding sites. Operators O_R, O_L, and O_D, recognized by the CI-NTD in TP901-1, homologous regions for φ13, and operators O_{R1}, O_{R2}, and O_{R3} for λ, are shown as blue arrows. Figure inspired by Pedersen et al. (2020)

performed with this protein preparation using fluorescent probes carrying O_R, O_L, or O_D from φ13 (Figure 2a). Agarose gel electrophoresis of binding reactions with increasing CI concentration followed by detection of the labeled DNA by fluorescence scanning showed that the rCI protein bound the O_L and O_D sites with high affinity (dissociation constants of 22 and 15 nM, respectively), but with lower affinity to the O_R site (dissociation constant of 310 nM) as shown in Figure 2b,c. While the operator half-sites of the O_L and O_D sequences correlated with the TP901-1 consensus (AGTTCAYR), one of the O_R half-sites deviated by one base (A<u>A</u>TTCATA). This difference could potentially explain the higher dissociation constant for binding to O_R. To validate that the putative binding sites were responsible for the binding to rCI, a series of mutated fluorescent DNA probes were produced, which were identical to the probes shown in Figure 2a, except that the central C nucleotide was mutated to G. Binding of rCI to these mutated control probes was severely weakened and no bands for specific binding could be detected (Figure 2b).
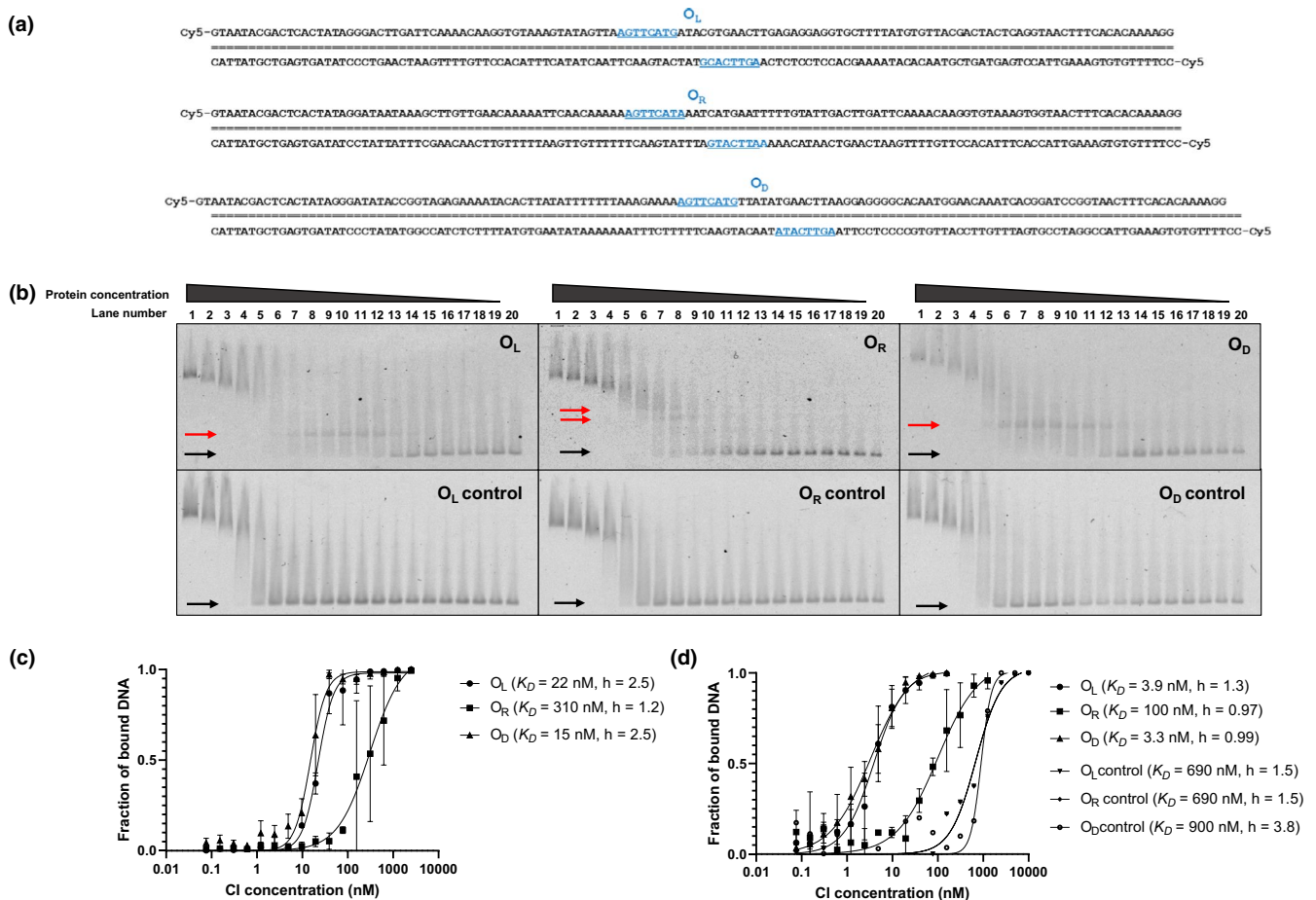
Interestingly, it can be seen from Figure 2b, that the bands with CI-bound DNA probe (marked with red arrows) disappear at higher concentrations of CI. We hypothesize that this is due to multimerization of CI because the labeled DNA probe migrates slowly as a smeared band at very high CI concentrations (Lane 1 in all gels in Figure 2b). To evaluate if the secondary binding events affected the determination of the dissociations constants, we plotted the missing fraction of the free DNA probe (i.e., the fraction of DNA probe that was retarded by any means) against the CI-concentration. Using this quantification method, the apparent dissociation constants for CI binding to the O_L, O_D, and O_R probes were found to be 3.9, 3.3, and 100 nM, respectively (Figure 2d), showing that the secondary binding events affected the determination of the dissociation constants. Also, the Hill coefficients for O_L and O_D binding were changed from 2.5 to 1.3 and 2.5 to 1.0, respectively (Figure 2c). The quantification of only the free DNA probe enabled the determination of apparent dissociation constants for binding of CI to the negative controls. Dissociation constants were detected at ~690, 900, and 690 nM, for the $O_L{}^{control}$, $O_D{}^{control}$, and $O_R{}^{control}$ probes, respectively, ten-fold and hundred-fold higher than the dissociation constants for the unmutated probes. In combination, these results show that the CI repressor from φ13 is functional and that the proposed operators are indeed binding sites for the repressor. The dissociation constants are somewhat lower than for binding of TP901-1 CI to DNA containing TP901-1 operators, found by mobility shift assays (Johansen et al., 2003; Pedersen & Hammer, 2008), but recent mobility shift assays of TP901-1 CI binding to O_L using the same technique employed in this study quantified the dissociation constant to 2.9 nM (Pedersen et al., 2020). It is important to mention that the binding of CI to O_R has introduced some interesting challenges. Preliminary analysis of operator binding to the O_L, O_D, and O_R operators using purified CI, in which the His-TEV-tag had been cleaved off, showed a dissociation constant that was slightly higher than shown above for binding to probes containing the O_L and O_D operators (~12 nM). Of more importance, the binding of the O_R probe to this CI fraction showed dissociation constants equaling the O_L and O_D operators (12 nM). This issue needs to be addressed in a future study, but the results obtained here and presented in Figure 2 have established that the proposed O_L, O_D, and O_R operators are specific binding sites for the φ13 CI repressor.

3.3 | A minimal 1.3 kb switch region from φ13 is capable of decision switching in *S. aureus*

After having shown that the *cI* encoded repressor can bind to an operator (O_L) overlapping the putative P_L promoter as in the TP901-1 switch, the isolation of a functional φ13 switch for in vivo analysis of switch frequencies appeared to be feasible. Previously a DNA fragment spanning the *cI* and *mor* genes from TP901-1 had successfully been inserted into a promoter fusion plasmid (Madsen et al., 1999), and used for detailed characterization of the TP901-1 switch (Pedersen & Hammer, 2008) through transformation of its *L. lactis* host. To monitor the regulatory decisions upon introduction of φ13 switch DNA, we constructed plasmids with transcriptional fusions to the P_L promoter of the φ13 switch region, as illustrated in Figure 3, with a *lacZ* reporter gene located after the *mor* gene. Upon transformation and plating on selective plates containing X-gal, the resulting colonies were either blue, indicative of high *mor* expression from the lytic P_L promoter, referred to as the "lytic" phenotype, or white, indicative of low *mor* expression due to repression of the P_L promoter by CI expressed from the lysogenic P_R promoter, referred to as the "lysogenic" phenotype.

Plasmid pCSK3 replicates in *S. aureus* and upon transformation of strain 8325-4 with pCSK3 we observed an average of 4.8% transformants with the "lysogenic" colony phenotype and 95% with the "lytic" phenotype (Table 4). This result indicated that the switch region present in pCSK3 could indeed perform decision switching in *S. aureus*. The genetic integrity of the switch region was verified by purification and subsequent re-transformation of pCSK3 isolated from 8325-4/pCSK3 transformants, yielding similar decision frequencies (see footnote to Table 4). Since the decision analysis was performed using a plasmid and not an intact phage, the use of pCSK3 as a model system for the φ13 decision switching required that the frequency of the "lysogenic" phenotype reflected the true lysogenization frequency. Infection of strain 8325-4 with the φ13-kana phage was therefore performed at a MOI of 1 and 0.1 at a bacterial concentration of 1.3×10^8 CFU ml^{-1}. As shown in Table A3, the average lysogenization frequency from five replicates was $4.6 \pm 2.8\%$ and $3.5 \pm 3.3\%$ for infections at an MOI of 1, and 0.1, respectively. Since the pCSK3 "lysogenic" (4.9%) and φ13 lysogenic frequencies are not significantly different ($p = 0.87$ and 0.47, for the two MOIs, respectively), we believe that the pCSK3 switch plasmid is a faithful biological model for φ13 switching. Finally, to ensure the importance of the MOR protein for the lytic pathway of the φ13 decision process, the start-codon in the *mor* gene was changed to a stop codon. The resulting plasmids, pCSK12, and pCSK13 acquired the "lysogenic" phenotype in 100% of transformations when introduced into *S. aureus* 8325-4, showing that the "lytic" phenotype is dependent upon the MOR protein (Table A4).

(a)

O_L

Cy5-GTAATACGACTCACTATAGGGACTTGATTCAAAACAAGGTGTAAAGTATAGTTAAGTTCATGATACGTGAACTTGAGAGGAGGTGCTTTTATGTGTTACGACTACTGAGGTAACTTTCACACAAAAGG
CATTATGCTGAGTGATATCCCTGAACTAAGTTTTGTTCCACATTTCATATCAATTCAAGTACTATGCACTTGAACTCTCCTCCACGAAAATACACAATGCTGATGAGTGCATTGAAAGTGTGTTTTCC-Cy5

O_R

Cy5-GTAATACGACTCACTATAGGATAATAAAAGCTTGTTGAACAAAAATTCAACAAAAAAGTTCATAAATCATGAATTTTTGTATTGACTTGATTCAAAACAAGGTGTAAAGTGGTAACTTTCACACAAAGG
CATTATGCTGAGTGATATCCTATTATTTCGAACAACTTGTTTTTAAGTTGTTTTTTCAAGTATTTAGTACTTAAAAACATAACTGAACTAAGTTTTGTTCCACATTTCACCATTGAAAGTGTGTTTTCC-Cy5

O_D

Cy5-GTAATACGACTCACTATAGGGATATACCGGTAGAGAAAATACACTTATATTTTTTAAAGAAAAAGTTCATGTTATATGAACTTAAGGAGGGGCACAATGGAACAAATCACGGATCCGGTAACTTTCACACAAAAGG
CATTATGCTGAGTGATATCCCTATATGGCCATCTCTTTTATGTGAATATAAAAAAATTTCTTTTTCAAGTACAATATACTTGAATTCCTCCCCGTGTTACCTTGTTTAGTGCCTAGGCCATTGAAAGTGTGTTTTCC-Cy5

(b)

Protein concentration ▸
Lane number 1 2 3 4 5 6 7 8 9 10 11 12 13 14 15 16 17 18 19 20   1 2 3 4 5 6 7 8 9 10 11 12 13 14 15 16 17 18 19 20   1 2 3 4 5 6 7 8 9 10 11 12 13 14 15 16 17 18 19 20

O_L   O_R   O_D

O_L control   O_R control   O_D control

(c)

Fraction of bound DNA vs CI concentration (nM)

- O_L (K_D = 22 nM, h = 2.5)
- O_R (K_D = 310 nM, h = 1.2)
- O_D (K_D = 15 nM, h = 2.5)

(d)

Fraction of bound DNA vs CI concentration (nM)

- O_L (K_D = 3.9 nM, h = 1.3)
- O_R (K_D = 100 nM, h = 0.97)
- O_D (K_D = 3.3 nM, h = 0.99)
- O_L control (K_D = 690 nM, h = 1.5)
- O_R control (K_D = 690 nM, h = 1.5)
- O_D control (K_D = 900 nM, h = 3.8)

FIGURE 2 EMSA of rCI repressor binding to putative operators O_R, O_L, and O_D in the φ13 switch. (a) Nucleotide sequence of the DNA fragments carrying φ13 O_L, O_R, and O_D. Operator sites are underlined in blue. (b) Fluorescent scan of agarose gels from EMSA employing φ13 rCI and DNA fragments carrying O_L, O_R, and O_D and of agarose gels from EMSA employing φ13 rCI and DNA fragments carrying mutated operator sites, in which the central C in each half-operator site was exchanged for a G: $O_R^{control}$, $O_L^{control}$, and $O_D^{control}$. Lane numbers are listed, where the concentration of rCI in lane 1 is 16.9 μM and in the following lanes diluted serially by two-fold dilutions. Lane 20 contains free unbound DNA. Black arrows point at bands with unbound DNA probe and red arrows point at bands for CI-bound DNA probe. Smears at high CI concentrations are presumed to be CI complexes bound to DNA probe. (c) Analysis of the degree of binding (CI-bound DNA/(unbound DNA + CI-bound DNA) from quantification of the bands for unbound DNA probe (black arrows in "b") and the bands for CI-bound DNA probe (red arrows in "b"), using the non-linear curve fitting option and the specific binding with Hill slope option in GraphPad Prism. Binding curves, dissociation constants, and Hill coefficients from the best fits are shown. Triplicate biological replicas were analyzed for the determination of specific binding and standard deviations from these are shown. (d) Analysis of the degree of binding calculated as (DNA in lane 20 – free DNA)/DNA in lane 20) from quantification of only the bands for unbound DNA probe (black arrows in b). Binding curves, dissociation constants, and Hill coefficients from the best fits are shown. Triplicate biological replica was analyzed for the determination of specific binding, and error bars represent ±one standard deviation

To analyze whether the decision frequency of the φ13 switch was dependent upon replication of the plasmid containing the switch DNA during the decision process, we introduced the switch on an integrative plasmid, pCSK9. Plasmid integration occurs at the bacterial attachment site of the phage L54a located in the lipase gene *geh* of *S. aureus* and is catalyzed by the phage integrase provided by plasmid pYL112-19 (Luong & Lee, 2007). Transformation of *S. aureus* 8325-4 with pCSK9 yielded a higher number of "lysogenic" colonies than with pCSK3 (12% compared to 4.9%, see Table 4). However, the very low efficiency of transformation (in total 77 transformants from 5 individual transformations) resulted in a high degree of variation, preventing a reliable determination of the decision frequency.

Despite this, the transformations permitted the isolation of pCSK9 transformants with both the "lysogenic" (CSK48) and "lytic" (CSK47) colony phenotype.

3.4 | The "lysogenic" colony phenotype from switch plasmids confers φ13 immunity

To assess whether the "lysogenic" colony phenotype expressed from the switch plasmids was functionally equivalent with the immunity derived from the φ13 prophages, we first tested if a φ13 lysogen could influence the decision frequency of the switch plasmids. To
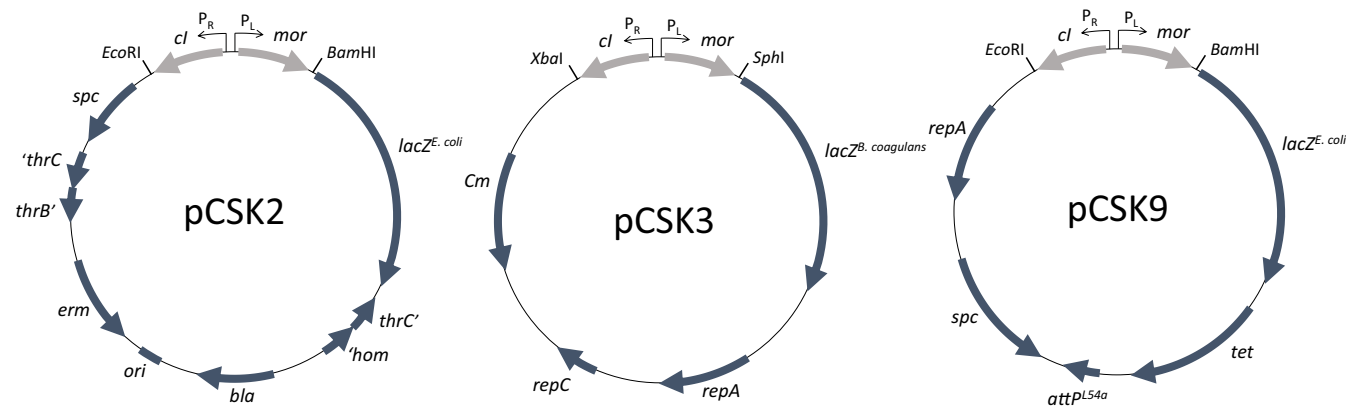
FIGURE 3 Reporter plasmids for monitoring switching of the φ13 switch in *B. subtilis* and *S. aureus*. The genetic switch of φ13 was inserted into the reporter plasmids pDG1729 (pCSK2), pNZlac (pCSK3), and pCL25 (pCSK9), allowing expression of the *lacZ* reporter gene at P_L activity. pCSK3 is capable of replication in *B. subtilis*, while pCSK2 lacks a replicon and needs to integrate by homologous recombination into the *thrC* gene of *B. subtilis*. pCSK9 integrates into the *attB*^L54a integration site in *S. aureus*, facilitated by a L54a integrase supplied by pYL112Δ19. Plasmid maps are not to scale. Restriction sites used for insertion of the switch DNA are shown. *cI* and *mor* of the φ13 genetic switch are illustrated in a lighter gray. Other contained genes: *spc*: spectinomycin resistance not expressed in *S. aureus*, *lacZ*^E. coli: beta-galactosidase gene originating from *E. coli* fused to the ribosome binding site of *B. subtilis spoVG*, '*hom, thrC*', '*thrC*, and *thrB*': segments of the genes flanking the integration site of pCSK2 in *B. subtilis* allowing integration by homologous recombination, *LacZ*^B. coagulans: beta-galactosidase gene originating from *B. coagulans*, *repA* and *repC*: replicon A and C, *Cm*: chloramphenicol resistance gene, *tet*: tetracycline resistance, *attP*^L54a: L54a phage attachment region

this end, pCSK3 and pCSK9 were introduced by transformation into (immune) *S. aureus* carrying a fully functional derivative of φ13 containing a kanamycin resistance gene (8325-4 φ13-kana) integrated into the chromosome (Tang et al., 2017). Despite a small number of successful transformation events (63 transformants from 9 individual transformations), which prevented reliable quantification of the switching frequency, it was striking that we exclusively observed "lysogenic" transformants when the φ13-kana lysogen was transformed with pCSK9 (Table 4, column 4), suggesting that the production of CI by the φ13 lysogen had influenced the decision process by pCSK9. Accordingly, the vast majority (99.6%) of pCSK3 transformants of *S. aureus* 8425-4 φ13-kana were "lysogenic" on X-gal-containing plates, showing a strong influence of lysogenic levels of CI on the decision by pCSK3. Interestingly, a small fraction of 0.4% established the "lytic" phenotype despite the presence of the φ13 prophage, verified by PCRs and kanamycin resistance. To analyze whether the switch or the reporter gene had mutated, plasmids were purified from the colonies that had escaped the immunity phenotype. Transformation of these plasmids into 8325-4 with and without the φ13 prophage yielded decision frequencies similar to the original transformations (see footnote to Table 4), showing that the "lytic" colony phenotype was not a result of mutations.

We then investigated whether the plasmid-derived "lysogenic" phenotype could confer φ13 immunity upon infection (Figure 4). When a liquid culture of the "lysogenic" 8325-4/pCSK3 (CSK33) was infected with φ13-kana, the "lysogenic" phenotype was found to restrict the production of phages (compare "B" and "E" in Figure 4). The same result was found when a transformant carrying the integrated pCSK9 plasmid (8325-4 *geh*::pCSK9, CSK48) was inoculated from a "lysogenic" colony and was infected with φ13-kana (compare "A" and "C" in Figure 4), showing that CI expressed from a chromosomally

integrated φ13 switch conferred immunity to attacking φ13 phages. When cells with the integrated switch plasmid were inoculated from a "lytic" colony and infected with φ13, the presence of the switch did not affect phage production (compare "A" and "D" in Figure 4). Surprisingly, however, when cells containing the replicative plasmid pCSK3 were inoculated from a "lytic" colony and infected by φ13-kana, the "lytic" switch phenotype inhibited phage production (compare "B" and "F" in Figure 4). It has previously been shown that replicating switch plasmids of TP901-1 favoring P_L ("lytic" phenotype) resulted in partial immunity towards infecting phages (Madsen et al., 1999), in accordance with the present results. This suggests that, although there is not enough CI repressor present to repress P_L on the multi-copy switch plasmid, the concentration is still sufficient to prevent lytic phage development. Upon screening of kanamycin resistance in cells surviving φ13-kana infection, very few lysogenic cells were detected, showing that survival under these conditions is not due to the formation of φ13-kana lysogens. Thus, the multi-copy plasmid-derived "lytic" switch phenotype appears to inactivate phage development in either direction.

3.5 | Decision switching by the minimal switch region from φ13 does not require *S. aureus* host factors

As *E. coli* host factors are known to affect the integration and induction of phage λ (Roucourt & Lavigne, 2009), it was of interest to establish whether the φ13 switch can function independently of host factors. Switch plasmid pCSK3 has an origin of replication that is functional in most Gram-positive bacteria (Kovács et al., 2010), and we could therefore also examine φ13 switching in

TABLE 4 Frequencies of colonies with "lysogenic" phenotype after the introduction of φ13 switch plasmids into *S. aureus* or *B. subtilis* by transformation

S. aureus 8325-4		*S. aureus* 8325-4 φ13-kana		*B. subtilis* 168	
pCSK3[a]	pCSK9[b]	pCSK3[c]	pCSK9[b]	pCSK3	pCSK2
4.9% ± 2.9% (n = 6)	12% ± 10% (77 colonies in total, n = 5)	99.6% ± 0.5% (n = 4)	100% ± 0% (63 colonies in total, n = 9)	3.8% ± 1.6% (n = 10)	3.0% ± 1.6% (n = 18)

Note: Switch plasmids were replicative (pCSK3) or required integration into the host (pCSK9 in *S. aureus*, pCSK2 in *B. subtilis*). Recipient bacteria were naïve (*S. aureus* 8325-4 or *B. subtilis* 168) or φ13 lysogens (*S. aureus* 8325-4 φ13-kana). The number of biological replicates with more than 100 resulting colonies is stated in brackets. Frequencies of "lysogenic" transformant colonies on plates containing X-gal were calculated as the frequency between "lytic" and "lysogenic" in each transformation event and the average is shown here. Standard deviations are based on differences between each event.

[a]Re-transformation of 8325-4 by pCSK3 plasmids extracted from "lytic" and "lysogenic" colonies of 8325-4/pCSK3 yielded frequencies of "lysogenic" transformant colonies of 11% and 5%, respectively.

[b]Indicates <100 transformants obtained in each experiment. The number of "lytic" and "lysogenic" colonies obtained in total for all replicas followed by the total count of biological replicates (n) for each event are stated in brackets.

[c]Re-transformation of 8325-4 by pCSK3 plasmids extracted from "lytic" and "lysogenic" colonies of 8325-4 φ13-kana/pCSK3 yielded frequencies of "lysogenic" transformant colonies of 3% and 11%, respectively. When these plasmids were used to transform 8325-4 φ13-kana, 100% "lysogenic" transformants were obtained.
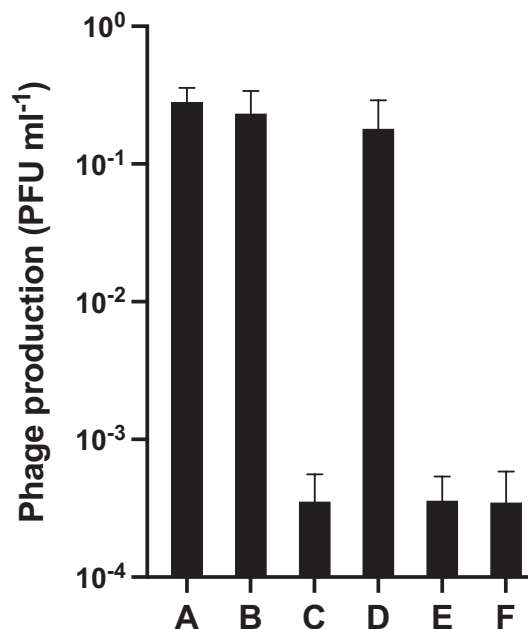

FIGURE 4 φ13-kana infection of *S. aureus* 8325-4 transformants carrying switch plasmids. Bacterial strains (A) 8325-4 *geh*::pCL25 (CSK68), (B) 8325-4/pNZlac (CSK59), (C) "lysogenic" 8325-4 *geh*::pCSK9 (CSK48), (D) "lytic" 8325-4 *geh*::pCSK9 (CSK47), (E) "lysogenic" 8325-4/pCSK3 (CSK33), and (F) "lytic" 8325-4/pCSK3 (CSK32) were infected by bacteriophage φ13-kana at a MOI of 0.1. Phage production was quantified by normalizing the number of phages (determined as PFU ml^{-1} of the culture supernatant 2 h after infection) by the CFU ml^{-1} of the bacterial culture before infection. (a) and (b) are controls where the strains contain the empty vectors used for the construction of pCSK9 and pCSK3, respectively. Bars represent the mean value of three replicate experiments, while error bars represent standard deviations

B. subtilis. As *B. subtilis* is a heterologous host, it carries no specific staphylococcal factors but contains general Gram-positive host factors. Upon transformation of pCSK3 into *B. subtilis* 168, we observed an average frequency of "lysogenic" colonies of 2%–3% (Table 4), which is close to the frequency obtained in *S. aureus*. This suggested that the decision frequency was not affected by specific host factors.

3.6 | Low spontaneous induction frequency from the "lysogenic" phenotype to the "lytic" phenotype

To examine the stability of the φ13 "lysogenic" colony switch phenotype, simulating the stability of φ13 lysogenic cells, we suspended and plated a large number of cells from "lysogenic" colonies on agar plates containing X-gal. Around 0.2% "lytic" colonies were detected in otherwise "lysogenic" colonies from both *B. subtilis* and *S. aureus*. This low level of toggling from the "lysogenic" to the "lytic" colony phenotype is hypothesized to be due to spontaneous induction of the SOS response, which is inevitable and leads to

prophage induction in bacteria that contain an SOS response and an intact *recA* gene (Goerke et al., 2006). To distinguish the process of toggle switching from a mutational event leading to the "lytic" colony phenotype, we purified pCSK3 plasmid from "lytic" spontaneous revertants and re-transformed them into the same host, with and without the φ13 prophage. After transformation of the strains with the extracted pCSK3 plasmid, we obtained a frequency of "lysogenic" transformant colonies at 5% for re-transformation of 8325-4, and at 100% for re-transformation 8325-4 φ13 kana, indistinguishable from frequencies obtained by transformation with the original plasmid, and showing that the change was epigenetic rather than mutational.

3.7 | High toggle frequency of the φ13 switch from the "lytic" to the "lysogenic" phenotype

While the "lysogenic" colony phenotype was very stable, the "lytic" colony phenotype was subject to frequent toggling to the "lysogenic" phenotype. When the cells from small (young) "lytic" colonies were suspended in medium and plated on agar plates containing X-gal, around 3% of the colonies had assumed the "lysogenic" phenotype. Plating of larger (older) "lytic" colonies resulted in an average of 60% "lysogenic" colonies. Because of the somewhat artificial nature of the "lytic" phenotype, the stability of the phenotype was not analyzed further.

3.8 | Induction of the "lytic" switch phenotype by DNA damaging agents

Above, we reported that 0.2% of cells that had grown in "lysogenic" colonies on an agar plate had spontaneously toggled to the "lytic" phenotype, possibly initiated by the spontaneous induction of the SOS response. A more dramatic visualization of the interplay between the DNA damage and the φ13 switch could be observed by exposing "lysogenic" cells to a gradient of DNA damaging agents on agar plates containing X-gal. Induction of "lysogenic" (white) to "lytic" (blue) toggle switching is intimately connected to the level of the DNA damaging compound as seen in Figure 5. In our working hypothesis, the cellular CI concentration is determined through a race between CI expression and CI degradation, where a threshold CI concentration has to be crossed if the switch should toggle from the "lysogenic" to the "lytic" phenotype. Two clear zones can be detected among the bacterial colonies on the X-gal-containing plates at different distances from the DNA damaging agents: a death zone and a toggle-inducing zone. The minimal inhibitory concentration (MIC) of the DNA damaging agent must be located at the border between growth and non-growth. Accordingly, a minimal toggle-inducing concentration (MTC) can be located at the border between purely white colonies and colonies with a bluish tint. For this analysis, a suspension of bacteria with the "lysogenic" (white) phenotype was plated on agar plates, and a drop of DNA damaging agent was applied to the center. Mitomycin C, ciprofloxacin, and hydrogen
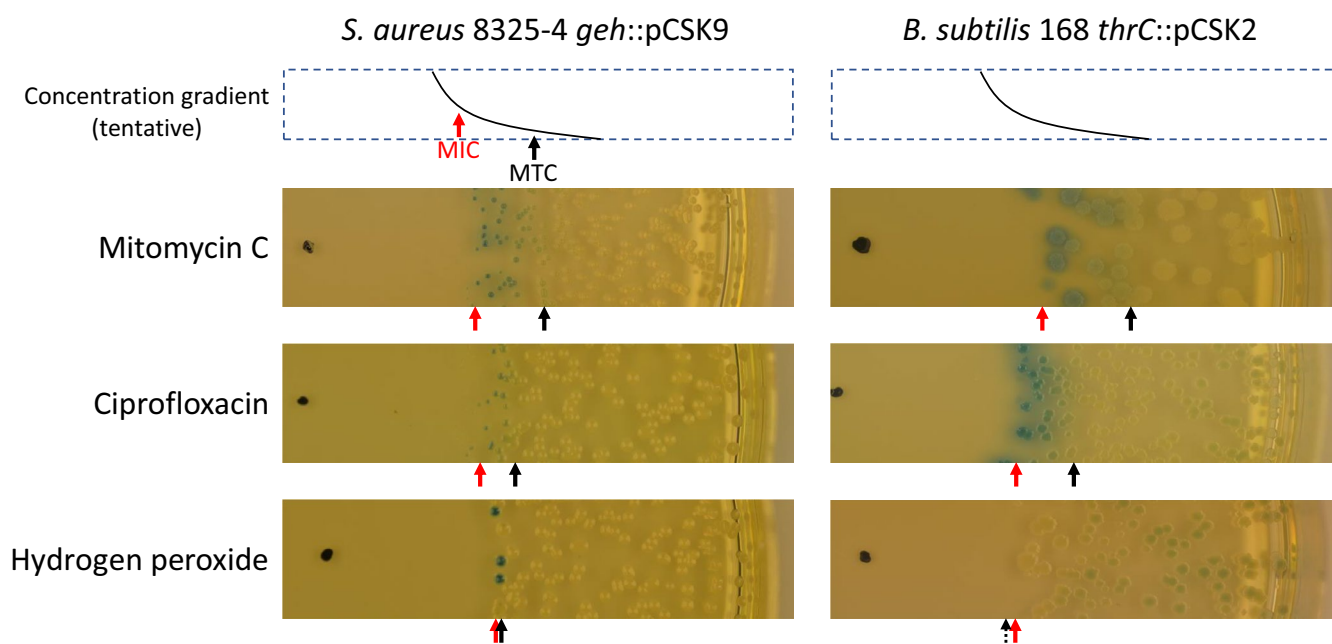

FIGURE 5 Induction of "lysogenic" transformants of *B. subtilis* 168 and *S. aureus* 8325-4 by mitomycin C, ciprofloxacin, and hydrogen peroxide. Bacteria from a "lysogenic" (white) colony of *S. aureus* 8325-4 *geh*::pCSK9 (CSK48, left) and *B. subtilis* 168 *thrC*::pCSK2 (CSK9, right) were suspended in media and plated on X-gal plates. After drying, a drop of mitomycin C (top), ciprofloxacin (middle), or hydrogen peroxide (bottom) was applied in the middle. The plate was incubated overnight at 37°C. Estimated MIC and MTC values are shown as red and black arrows, respectively. The MTC value of *B. subtilis* 168 *thrC*::pCSK2 exposed to hydrogen peroxide cannot be determined, but an estimate is suggested by a dashed arrow

peroxide are all known to induce φ13 lysogens (Goerke, Koller, et al., 2006; Tang et al., 2017), and Figure 5 shows the response of the φ13 switch plasmid to gradients of DNA damaging agents in its natural host (Figure 5, left panel, 8325-4 *geh*::pCSK9 (CSK48)) and in *B. subtilis* (Figure 5, right panel, 168 *thrC*::pCSK2 (CSK9)). In all cases, a sharp boundary (MIC) was formed, where no cells could grow inside the boundary, but where colonies could be formed in the sub-MIC concentrations outside the boundary.

Mitomycin C and ciprofloxacin exposure resulted in very similar induction patterns in both *S. aureus* and *B. subtilis* hosts. The colony phenotypes showed a wide toggle-inducing zone where a varying fraction of cells had switched to a "lytic" (blue) phenotype (top four panels in Figure 5). Hydrogen peroxide showed an extremely thin toggle-inducing zone for the *S. aureus* host but no toggle-inducing zone at all for the *B. subtilis* host (bottom panels in Figure 5). The difference in induction pattern most likely reflects that the MTC for hydrogen peroxide is higher than the MIC value in *B. subtilis*, but that MTC and MIC are almost equal in *S. aureus*. For mitomycin C and ciprofloxacin, the MTC value is significantly lower than the MIC value in both hosts.

Across the toggle-inducing zone of mitomycin C and ciprofloxacin the intensity of blue color decreases (top four panels in Figure 5), likely due to smaller fractions of toggle-switched cells in the colonies. To quantify the fractions of stable toggle-switched cells, we picked colonies grown at known distances from an application spot containing mitomycin C and determined the fraction of cells in each colony that could form colonies with a stable "lytic" phenotype. After a suspension of each colony in a fresh medium, plating, incubation, and quantifying the fraction of "lytic" colonies, an exponential dependency was observed between the frequency of "lytic" cells and the distance to the application spot for both *S. aureus* and *B. subtilis* (Figure 6). This could suggest a quasi-linear dependence between the toggle switch frequency and the mitomycin C concentration since we expect a similar decrease in concentration by diffusion of a compound in agar (Koch, 1999), although the inherent instability of the "lytic" phenotype detected above should be taken into consideration. This dependence of toggle frequency on the concentration of the DNA damaging agent suggests the existence of high stochasticity in either the level of DNA damage, the concentration of RecA* nucleofilaments, the rate of autocleavage of CI, or the competition
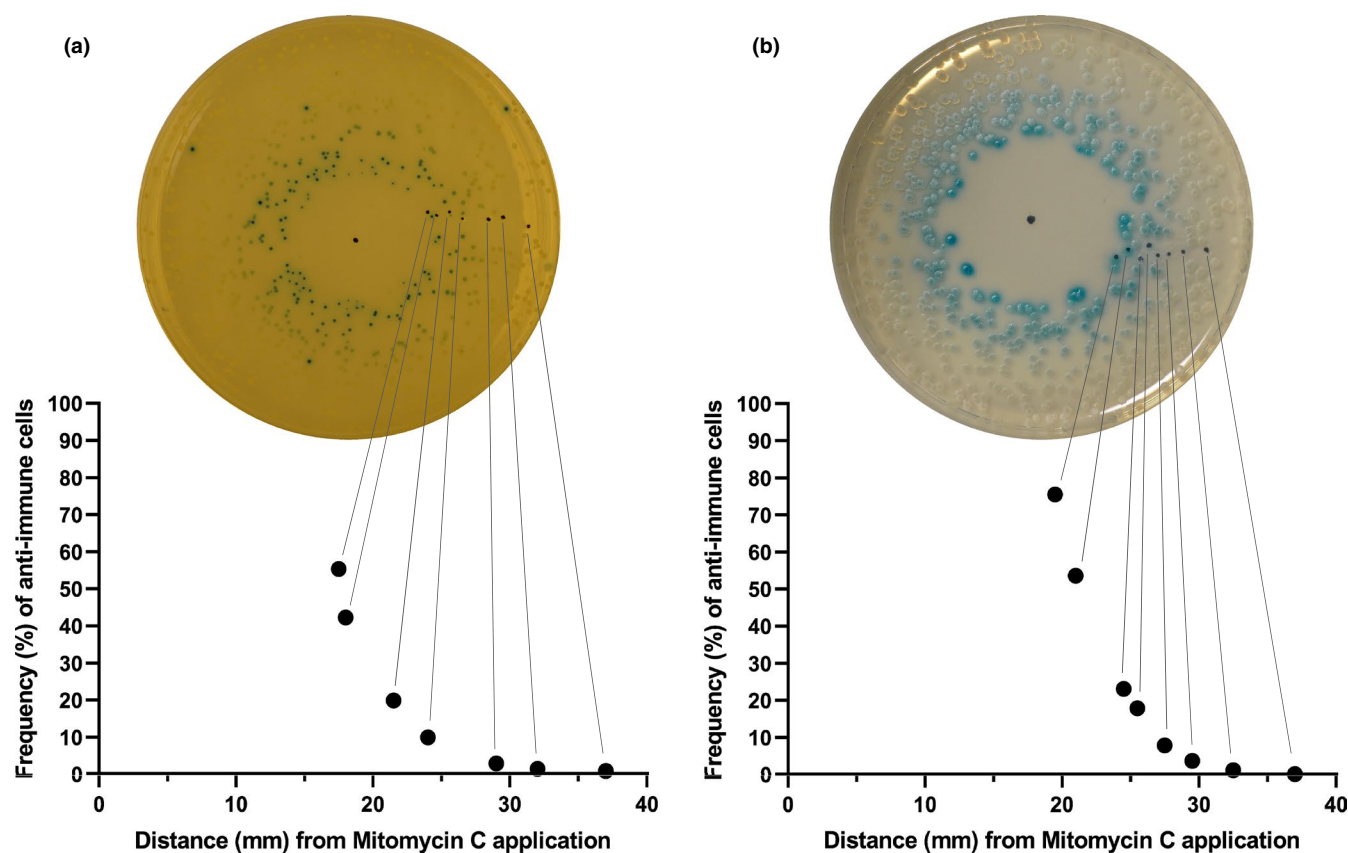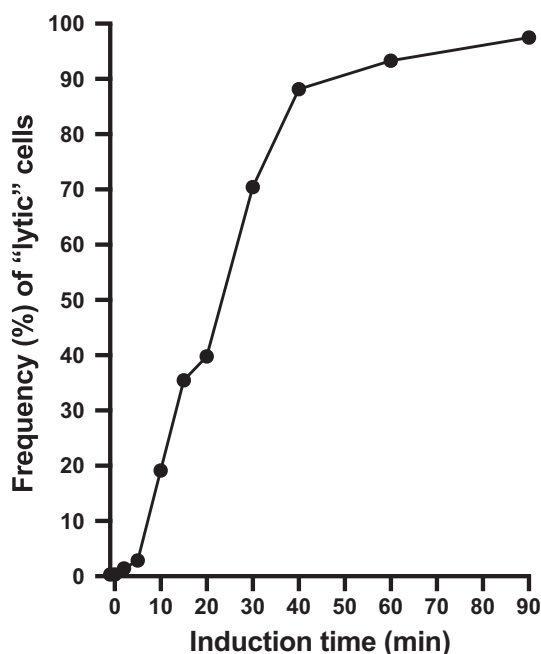

FIGURE 6 Toggle switching of "lysogenic" cells in response to mitomycin C. Bacteria from a "lysogenic" (white) transformant of (a) 8325-4 *geh*::pCSK9 (CSK48) and (b) *B. subtilis* 168 *thrC*::pCSK2 (CSK9) were plated, and a small drop of mitomycin C was immediately placed in the center. After growth overnight, individual colonies at different distances to the mitomycin C application spots were picked and suspended in medium without mitomycin C, from which dilutions were plated on LB/TSA X-gal plates. The frequency of colonies with the "lytic" (blue) phenotype was determined and plotted against the distance to the mitomycin C application. Lines have been inserted to illustrate the relationship between colonies on the plates and the determined frequencies of toggle switching

between the elements in the φ13 switch. Experiments to unravel the kinetic relationship between induction of the SOS response and the toggle switching of the genetic switch would be interesting, but it would require simultaneous monitoring of the SOS response.

3.9 | Timing of commitment to the "lytic" phenotype in *S. aureus*

To examine the timing of the response of the switch to DNA damage, we exposed "lysogenic" 8325-4 *geh*::pCSK9 (CSK48) cells to mitomycin C at a final concentration of 1 µg ml^{-1}. Induction of toggle switch to the "lytic" phenotype was monitored by plating dilutions of the mitomycin C treated culture on TSA plates containing X-gal. A "lytic" phenotype indicated that the induced cell that formed the colony was committed to the "lytic" phenotype and had passed on the phenotype to the descendants in the colony. Figure 7 shows the temporal increase in the fraction of cells committed to forming colonies with a stable "lytic" phenotype (in percent). The highest frequency of commitment to the "lytic" phenotype was obtained between 5 and 40 min of exposure to mitomycin C, and as many as 30% of all cells became dedicated in 20–30 min. However, because of the stochastic nature of the induction process, a fraction of the bacteria showed commitment in <5 min of exposure to mitomycin C (3% of

FIGURE 7 Induction of "lysogenic" to "lytic" toggle switching from pCSK9 plasmids in *S. aureus* by temporal exposure to mitomycin C. "Lysogenic" 8325-4 *geh*::pCSK9 (CSK48) cells were grown in liquid TSB medium (in duplicates) and induced by addition of 1 µg ml^{-1} mitomycin C at time = 0 min. At the indicated times, aliquots were harvested and dilutions were plated on TSA plates containing X-gal. The average fraction of colonies (in percent) with the "lytic" phenotype was plotted against the duration (in min) of the exposure to mitomycin C

the cells), while other cells required exposure for more than 40 min before commitment (10% of the cells). As discussed above, the CI threshold allowing toggle switching is determined by many factors, such as the extent of DNA damage, the CI degradation rate, the CI synthesis rate, and φ13 switch kinetics, each adding to the overall stochasticity of the process.

4 | CONCLUSIONS

In this study, we have reported the first analysis of a genetic switch from a Sa3int bacteriophage with implications for the phage-derived host specificity of *S. aureus* bacteria towards humans. As identical switches are present in other Sa3int phages and unrelated phages carrying genes for PVL, the results are also relevant for a larger group of pathogenic phages. Inhibition of the process leading to phage integration into *S. aureus* hosts could influence their ability to colonize humans. Therefore, it is crucial to understand the process by which the phage switch decides between (i) lysogenization of the host to integrate as a prophage or (ii) multiplying and killing of the host. It is equally important to understand the toggle process that induces a Sa3int prophage to kill the bacterium and release a litter of newly produced phages. We have shown that a minimal genetic switch of φ13, contained on a 1.3 kb DNA fragment and expressing functional *cI* and/or *mor* genes from divergent promoters, is fully competent in both decision switching and toggle switching. Purified his-tagged CI protein was found to be folded, stable, and to bind with high affinity to operators with two half-sites following the AGTTCAYR consensus, but with low affinity to mutant operators (AGTT**G**AYR). The two alternative phenotypes of the epigenetic switch are not equally stable. While the "lysogenic" phenotype is very stable (although chosen in <5% of the decision events) and leads to the lysogenic life cycle of the phage, the frequent "lytic" phenotype that resembles the first phase in the lytic life cycle is unstable and toggles towards the "lysogenic" phenotype. If this high toggle frequency indicates that prophage induction may be reversible in its early phase, then our preliminary findings that the nutritional status of the cell can modulate the toggle frequency could prove relevant.

Induction of "lysogenic" to "lytic" toggling by DNA damaging agents, resembling the induction of the φ13 prophage, was visualized in a plate diffusion assay that enabled us to locate MIC and MTC values (Figure 5). In this work, we defined MTC values as a tool to distinguish between the antibiotic killing of cells by inhibition of cell function from killing by induction of phage lysis. Relative MIC/MTC ratios could be important in the clinical use of DNA damaging antibiotics to prevent phage lysis mediated toxin production (Zhang et al., 2000) or production of host transforming phages like φ13. Antibiotics with a MIC/MTC ratio below 1.0 would be safe in this regard; however, as shown for hydrogen peroxide (Figure 5), the MIC/MTC ratio can be strain or species-specific. Timing of the induction process revealed a highly stochastic process with a maximal toggling rate, leading to dedicated cells with the stable "lytic" phenotype, between 20 and 30 min of exposure to mitomycin C. While

the induction of DNA damage in each cell ultimately defines a particular CI degradation rate, this could easily be changing over time due to the SOS induction of DNA repair enzymes. The stochasticity of the toggle frequency at different time points could originate at many levels, including the initial CI and MOR concentrations, their production levels, and the DNA damage-induced CI degradation rate. While toggle switching has been reported for many bistable switches (Dubnau & Losick, 2006), the ability of an isolated switch to conduct both decision switching and toggle switching has not previously been demonstrated for any phage.

ETHICS STATEMENT

None required.

CONFLICT OF INTEREST

None declared.

AUTHOR CONTRIBUTIONS

Camilla Schoopp Kristensen: Conceptualization (equal); Data curation (lead); Investigation (lead); Methodology (equal); Validation (equal); Visualization (equal); Writing-original draft (equal); Writing-review & editing (equal). **Anders Kokkenborg Varming:** Data curation (supporting); Formal analysis (supporting); Investigation (supporting); Writing-review & editing (equal). **Helena Augusta Katharina Leinweber:** Investigation (supporting); Supervision (supporting); Writing-review & editing (equal). **Karin Hammer:** Conceptualization (supporting); Methodology (supporting); Validation (supporting); Writing-original draft (supporting); Writing-review & editing (equal). **Leila Lo Leggio:** Conceptualization (supporting); Data curation (supporting); Formal analysis (supporting); Funding acquisition (equal); Methodology (supporting); Supervision (supporting); Validation (supporting); Writing-original draft (supporting); Writing-review & editing (equal). **Hanne Ingmer:** Conceptualization (supporting); Funding acquisition (equal); Supervision (equal); Writing-original draft (supporting); Writing-review & editing (equal). **Mogens Kilstrup:** Conceptualization (lead); Data curation (equal); Investigation (equal); Methodology (equal); Project administration (lead); Supervision (lead); Visualization (equal); Writing-original draft (equal); Writing-review & editing (equal).

DATA AVAILABILITY STATEMENT

The data generated and analyzed during the current study are available in the Zenodo repository at https://doi.org/10.5281/zenodo.5515850

ORCID

Camilla S. Kristensen https://orcid.org/0000-0001-6564-8455
Anders K. Varming https://orcid.org/0000-0001-6865-990X
Helena A. K. Leinweber https://orcid.org/0000-0002-9949-819X
Karin Hammer https://orcid.org/0000-0002-6250-8067
Leila Lo Leggio https://orcid.org/0000-0002-5135-0882
Hanne Ingmer https://orcid.org/0000-0002-8350-5631
Mogens Kilstrup https://orcid.org/0000-0002-3900-723X

REFERENCES

Altschul, S. F., Gish, W., Miller, W., Myers, E. W., & Lipman, D. J. (1990). Basic local alignment search tool. *Journal of Molecular Biology*, *215*(3), 403–410. https://doi.org/10.1016/S0022-2836(05)80360-2

Atsumi, S., & Little, J. W. (2006). Role of the lytic repressor in prophage induction of phage λ as analyzed by a module-replacement approach. *Proceedings of the National Academy of Sciences of the United States of America*, *103*(12), 4558–4563. https://doi.org/10.1073/pnas.0511117103

Burkholder, P. R., & Giles, N. H. (1947). Induced biochemical mutations in *Bacillus subtilis*. *American Journal of Botany*, *34*(6), 345–348. https://doi.org/10.2307/2437147

Casjens, S. R., & Hendrix, R. W. (2015). Bacteriophage lambda: Early pioneer and still relevant. *Virology*, *479-480*, 310–330. https://doi.org/10.1016/j.virol.2015.02.010

Coleman, D., Knights, J., Russell, R., Shanley, D., Birkbeck, T. H., Dougan, G., & Charles, I. (1991). Insertional inactivation of the *Staphylococcus aureus* β-toxin by bacteriophage φ13 occurs by site-and orientation-specific integration of the φ13 genome. *Molecular Microbiology*, *5*(4), 933–939. https://doi.org/10.1111/j.1365-2958.1991.tb00768.x

Dubnau, D., & Losick, R. (2006). Bistability in bacteria. *Molecular Microbiology*, *61*(3), 564–572. https://doi.org/10.1111/j.1365-2958.2006.05249.x

Gardner, T. S., Cantor, C. R., & Collins, J. J. (2000). Construction of a genetic toggle switch in *Escherichia coli*. *Nature*, *403*(6767), 339–342. https://doi.org/10.1038/35002131

Gasteiger, E., Hoogland, C., Gattiker, A., Duvaud, S., Wilkins, M. R., Appel, R. D., & Bairoch, A. (2005). Protein identification and analysis tools on the ExPASy server. In J. M. Walker (Eds.), *The proteomics protocols handbook* (pp. 571–608). Humana Press.

Goerke, C., Koller, J., & Wolz, C. (2006). Ciprofloxacin and trimethoprim cause phage induction and virulence modulation in *Staphylococcus aureus*. *Antimicrobial Agents and Chemotherapy*, *50*(1), 171–177. https://doi.org/10.1128/AAC.50.1.171-177.2006

Goerke, C., Pantucek, R., Holtfreter, S., Schulte, B., Zink, M., Grumann, D., Bröker, B. M., Doskar, J., & Wolz, C. (2009) Diversity of prophages in dominant *Staphylococcus aureus* clonal lineages. *Journal of Bacteriology*, *191*(11), 3462–3468. https://doi.org/10.1128/JB.01804-08

Goerke, C., Wirtz, C., Fluckiger, U., & Wolz, C. (2006). Extensive phage dynamics in *Staphylococcus aureus* contributes to adaptation to the human host during infection. *Molecular Microbiology*, *61*(6), 1673–1685. https://doi.org/10.1111/j.1365-2958.2006.05354.x

Grodzicker, T., Arditti, R. R., & Eisen, H. (1972). Establishment of repression by lambdoid phage in catabolite activator protein and adenylate cyclase mutants of *Escherichia coli*. *Proceedings of the National Academy of Sciences of the United States of America*, *69*(2), 366–370. https://doi.org/10.1073/pnas.69.2.366

Guérout-Fleury, A. M., Frandsen, N., & Stragier, P. (1996). Plasmids for ectopic integration in *Bacillus subtilis*. *Gene*, *180*(1–2), 57–61. https://doi.org/10.1016/S0378-1119(96)00404-0

Herman, C., Ogura, T., Tomoyasu, T., Hiraga, S., Akiyama, Y., Ito, K., Thomas, R., D'Ari, R., & Bouloc, P. (1993). Cell growth and λ phage

development controlled by the same essential *Escherichia coli* gene, *ftsH/hflB*. *Proceedings of the National Academy of Sciences of the United States of America*, *90*(22), 10861–10865. https://doi.org/10.1073/pnas.90.22.10861

Huseby, M., Shi, K., Brown, C. K., Digre, J., Mengistu, F., Seo, K. S., Bohach, G. A., Schlievert, P. M., Ohlendorf, D. H., & Earhart, C. A. (2007). Structure and biological activities of beta toxin from *Staphylococcus aureus. Journal of Bacteriology*, *189*(23), 8719–8726. https://doi.org/10.1128/JB.00741-07

Ingmer, H., Gerlach, D., & Wolz, C. (2019). Temperate phages of *Staphylococcus aureus. Microbiology Spectrum*, *7*(5), https://doi.org/10.1128/microbiolspec.gpp3-0058-2018

Johansen, A. H., Brøndsted, L., & Hammer, K. (2003). Identification of operator sites of the CI repressor of phage TP901-1: Evolutionary link to other phages. *Virology*, *311*(1), 144–156. https://doi.org/10.1016/S0042-6822(03)00169-7

Katayama, Y., Baba, T., Sekine, M., Fukuda, M., & Hiramatsu, K. (2013). Beta-hemolysin promotes skin colonization by *Staphylococcus aureus. Journal of Bacteriology*, *195*(6), 1194–1203. https://doi.org/10.1128/JB.01786-12

Kihara, A., Akiyama, Y., & Ito, K. (2001). Revisiting the lysogenization control of bacteriophage λ. Identification and characterization of a new host component, HflD. *Journal of Biological Chemistry*, *276*(17), 13695–13700. https://doi.org/10.1074/jbc.M011699200

Koch, A. L. (1999). Diffusion through agar blocks of finite dimensions: A theoretical analysis of three systems of practical significance in microbiology. *Microbiology*, *145*(3), 643–654. https://doi.org/10.1099/13500872-145-3-643

Konkol, M. A., Blair, K. M., & Kearns, D. B. (2013). 'Plasmid-encoded ComI inhibits competence in the ancestral 3610 strain of *Bacillus subtilis. Journal of Bacteriology*, *195*(18), 4085–4093. https://doi.org/10.1128/JB.00696-13

Kovács, A. T., van Hartskamp, M., Kuipers, O. P., & van Kranenburg, R. (2010). Genetic tool development for a new host for biotechnology, the thermotolerant bacterium *Bacillus coagulans. Applied and Environmental Microbiology*, *76*(12), 4085–4088. https://doi.org/10.1128/AEM.03060-09

Lee, C. Y., Buranen, S. L., & Zhi-Hai, Y. (1991). Construction of single-copy integration vectors for *Staphylococcus aureus. Gene*, *103*(1), 101–105. https://doi.org/10.1016/0378-1119(91)90399-V

Little, J. W. (1984). Autodigestion of *lexA* and phage λ repressors. *Proceedings of the National Academy of Sciences of the United States of America*, *81*(3I), 1375–1379. https://doi.org/10.1073/pnas.81.5.1375

Liu, G. Y. (2009). Molecular pathogenesis of *Staphylococcus aureus* infection. *Pediatric Research*, *65*, 71R–77R. https://doi.org/10.1203/PDR.0b013e31819dc44d

Lowy, F. D. (1998). *Staphylococcus aureus* infections. *New England Journal of Medicine*, *339*(8), 520–532. https://doi.org/10.1056/NEJM199808203390806

Luong, T. T., & Lee, C. Y. (2007). Improved single-copy integration vectors for *Staphylococcus aureus. Journal of Microbiological Methods*, *70*(1), 186–190. https://doi.org/10.1016/j.mimet.2007.04.007

Madsen, P. L., Johansen, A. H., Hammer, K., & Brøndsted, L. (1999). 'The genetic switch regulating activity of early promoters of the temperate lactococcal bacteriophage TP901-1. *Journal of Bacteriology*, *181*(24), 7430–7438. https://doi.org/10.1128/jb.181.24.7430-7438.1999

Micsonai, A., Wien, F., Bulyáki, É., Kun, J., Moussong, É., Lee, Y.-H., Goto, Y., Réfrégiers, M., & Kardos, J. (2018). BeStSel: A web server for accurate protein secondary structure prediction and fold recognition from the circular dichroism spectra. *Nucleic Acids Research*, *46*(W1), W315–W322. https://doi.org/10.1093/nar/gky497

Micsonai, A., Wien, F., Kernya, L., Lee, Y.-H., Goto, Y., Réfrégiers, M., & Kardos, J. (2015). Accurate secondary structure prediction and fold recognition for circular dichroism spectroscopy. *Proceedings of the National Academy of Sciences of the United States of America*,

112(24), E3095–E3103. https://doi.org/10.1073/pnas.1500851112

Monk, I. R., Tree, J. J., Howden, B. P., Stinear, T. P., & Foster, T. J. (2015). Complete bypass of restriction systems for major *Staphylococcus aureus* lineages. *MBio*, *6*(3), 1–12. https://doi.org/10.1128/mBio.00308-15

Novick, R. P. (1963). Analysis by transduction of mutations affecting penicillinase formation. *Journal of General Microbiology*, *33*(1), 121–136. https://doi.org/10.1099/00221287-33-1-121

Novick, R. (1967). Properties of a cryptic high-frequency transducing phage in *Staphylococcus aureus. Virology*, *33*(1), 155–166. https://doi.org/10.1016/0042-6822(67)90105-5

Oliveira, H., Sampaio, M., Melo, L. D. R., Dias, O., Pope, W. H., Hatfull, G. F., & Azeredo, J. (2019). Staphylococci phages display vast genomic diversity and evolutionary relationships. *BMC Genomics*, *20*, 357. https://doi.org/10.1186/s12864-019-5647-8

Oppenheim, A. B., Kobiler, O., Stavans, J., Court, D. L., & Adhya, S. (2005). Switches in bacteriophage lambda development. *Annual Review of Genetics*, *39*(1), 409–429. https://doi.org/10.1146/annurev.genet.39.073003.113656

Pedersen, M., & Hammer, K. (2008). The role of MOR and the CI operator sites on the genetic switch of the temperate bacteriophage TP901-1. *Journal of Molecular Biology*, *384*(3), 577–589. https://doi.org/10.1016/j.jmb.2008.09.071

Pedersen, M., Neergaard, J. T., Cassias, J., Rasmussen, K. K., Lo Leggio, L., Sneppen, K., Hammer, K., & Kilstrup, M. (2020). Repression of the lysogenic PR promoter in bacteriophage TP901-1 through binding of a CI-MOR complex to a composite OM-OR operator. *Scientific Reports*, *10*(1), 8659. https://doi.org/10.1038/s41598-020-65493-0

Riva, S., Polsinelli, M., & Falaschi, A. (1968). A new phage of *Bacillus subtilis* with infectious DNA having separable strands. *Journal of Molecular Biology*, *35*(2), 347–356. https://doi.org/10.1016/S0022-2836(68)80029-4

Roucourt, B., & Lavigne, R. (2009). The role of interactions between phage and bacterial proteins within the infected cell: A diverse and puzzling interactome. *Environmental Microbiology*, *11*(11), 2789–2805. https://doi.org/10.1111/j.1462-2920.2009.02029.x

Salgado-Pabón, W., Herrera, A., Vu, B. G., Stach, C. S., Merriman, J. A., Spaulding, A. R., & Schlievert, P. M. (2014). *Staphylococcus aureus* β-toxin production is common in strains with the β-toxin gene inactivated by bacteriophage. *Journal of Infectious Diseases*, *210*(5), 784–792. https://doi.org/10.1093/infdis/jiu146

Schindelin, J., Arganda-Carreras, I., Frise, E., Kaynig, V., Longair, M., Pietzsch, T., Preibisch, S., Rueden, C., Saalfeld, S., Schmid, B., Tinevez, J.-Y., White, D. J., Hartenstein, V., Eliceiri, K., Tomancak, P., & Cardona, A. (2012). Fiji: An open-source platform for biological-image analysis. *Nature Methods*, *9*(7), 676–682. https://doi.org/10.1038/nmeth.2019

Sreerama, N., & Woody, R. W. (2000). Estimation of protein secondary structure from circular dichroism spectra: Comparison of CONTIN, SELCON, and CDSSTR methods with an expanded reference set. *Analytical Biochemistry*, *287*(2), 252–260. https://doi.org/10.1006/abio.2000.4880

Tang, Y., Nielsen, L. N., Hvitved, A., Haaber, J. K., Wirtz, C., Andersen, P. S., Larsen, J., Wolz, C., & Ingmer, H. (2017). Commercial biocides induce transfer of prophage Φ13 from human strains of *Staphylococcus aureus* to livestock CC398. *Frontiers in Microbiology*, *8*, 2418. https://doi.org/10.3389/fmicb.2017.02418

Tong, S. Y. C., Davis, J. S., Eichenberger, E., Holland, T. L., & Fowler, V. G. (2015). *Staphylococcus aureus* infections: Epidemiology, pathophysiology, clinical manifestations, and management. *Clinical Microbiology Reviews*, *28*(3), 603–661. https://doi.org/10.1128/CMR.00134-14

Whitmore, L., & Wallace, B. A. (2008). Protein secondary structure analyses from circular dichroism spectroscopy: Methods and reference

databases. *Biopolymers*, *89*(5), 392–400. https://doi.org/10.1002/bip.20853

Xia, G., & Wolz, C. (2014). Phages of *Staphylococcus aureus* and their impact on host evolution. *Infection, Genetics and Evolution*, *21*, 593–601. https://doi.org/10.1016/j.meegid.2013.04.022

Zhang, X., McDaniel, A. D., Wolf, L. E., Keusch, G. T., Waldor, M. K., & Acheson, D. W. K. (2000). Quinolone antibiotics induce Shiga toxin-encoding bacteriophages, toxin production, and death in mice. *The Journal of Infectious Diseases*, *181*(2), 664–670. https://doi.org/10.1086/315239

APPENDIX

```
Phi13_CI-tagged     1 MKHHHHHHPMSDYDIPTTENLYFQGMREKVSNRLKHIMKIRNLKQVDIINKSKPYQKKLG

Phi13_CI-tagged    61 ISLSKSTLSQYINDVQSPDQDRIYLLSKTLNVGEAWLMGYDVDSYRVPDEERQDETIMSK

Phi13_CI-tagged   121 INNIFSQLTPPRQENVLNYANEQLEEQNKVTSIDGYKESKLVSYIACGATGAGIGEELYD

Phi13_CI-tagged   181 DILHEEVFFKEDETPSNADFCILVNGDSMEPMLKQGTYAFIKKEDSIKDGTIALVVLDGV

Phi13_CI-tagged   241 SLIKRVDICEDYINLVSLNPKYDDIKVASFSDIKVMGKVVL
```

FIGURE A1 The protein sequence of φ13 rCI used in this study. The added tag is marked with a black box and consists of the His-tag (HHHHHH) and a TEV cleavage site (ENLYFQG). Cleavage of the tag leaves the G

CI

NTD (DNA binding and MOR interaction)

```
TP901-1   MKTDTSNRLKQIMAERNLKQVDILNLSIPFQKKFGIKLSKSTLSQYVNSVQSPDQNRIYL    60
          M+     SNRLK IM  RNLKQVDI+N S P+QKK GI LSKSTLSQY+N VQSPDQ+RIYL
Φ13       MREKVSNRLKHIMKIRNLKQVDIINKSKPYQKKLGISLSKSTLSQYINDVQSPDQDRIYL    60
                        L Q  +           K+G+    +S +    N + + +      L
Lambda                 31-LSQESV-------ADKMGMG--QSGVGALFNGINALNAYNAAL    66
```
DNA binding (HTH)

CTD1 (dimer interface)

```
Tp901-1   LAKTLGVSEAWLMGFDVPMVESSKIENDSENIEETI-----TVMKKLEEPRQKVVLDTAK   115
          L+KTL V EAWLMG+D    V+S ++   D E  +ETI      + +L  PRQ+ VL+ A
Φ13       LSKTLNVGEAWLMGYD---VDSYRVP-DEERQDETIMSKINNIFSQLTPPRQENVLNYAN   116
          L+K L V                   P        R+           I+
Lambda    LAKILKVSVEEFS------------P-SIARE----------IY----------------    91
```

```
Tp901-1   IQLKEQDEQNKVKQIEDYRLSDEYLEEQISKASAYGGGQLND---NDKEFFKRLLKNTLK   172
           QL  +EQNKV  I+ Y+ S            A  G +L D    +++ FFK
Φ13       EQL---EEQNKVTSIDGYKESKLVSYIACGATGAGIGEELYDDILHEEVFFKEDETPSNA   173
                  +   S+    E + S++  G         E           E| +     +  S++
Lambda    --------VSMQPSLRSEYEYPVFSHVQAGMF---SPELRTFTKGDAERWVSTTKKASDS   139
```
auto cleavage site (between A and G)

```
Tp901-1   EKIDKGDL*                                                    180
```

```
Φ13       DFCILVNGDSME------PMLKQGTYAFIKKEDSIKDGTIALVVLDGVSL-IKRVDICED   226
          F + V G+SM        P       G    + E +++ G   + L G      K++
Lambda    AFWLEVEGNSMTAPTGSKPSFPDGMLILVDPEQAVEPGDFCIARLGGDEFTFKKLIRDSG   200
```
catalytic Ser   dimer interface   catalytic Lys

```
Φ13       YINLVSLNPKYDDIKVASFSDIKVMGKVVL*                              256
          + L   LNP+Y  I       V+GKV+
Lambda    QVFLQPLNPQYPMIPCN—ESCSVVGKVIASOWPEETFG*                      237
```
dimer interface

MOR

```
Tp901-1   MSYDYSSLLGKITEKCGTQYNFAIAMGLSERTVSLKLNDKVTWKDDEILKAVHVLELNPQ    60
          M YDYS L GKI EK GTQYNFAIAM LSER++SLKLN KV WKD EI KA+ +L++   +
Φ13       MCYDYSRLSGKIVEKYGTQYNFAIAMKLSERSLSLKLNGKVGWKDSEIWKAIQLLDIPVE    60
```

```
Tp901-1   DIPKYFFNAKVH                                                  72
           I  YFF  KVH
Φ13       KIHLYFFKEKVH                                                  72
```

FIGURE A2 Sequence alignments of CI from *L. lactis* phage TP901-1, *S. aureus* phage φ13, and *E. coli* phage λ (top) and MOR from TP901-1 and φ13 (bottom). Identical and similar residues are shown in gray. Known domains are indicated by lines and designated by brief descriptions. The overall similarity between the CI repressors from φ13 and TP901-1 is 51% identical residues, while the local domain similarity for the NTD and CTD_1 is 71% and 39%, respectively. The overall similarity between CI from φ13 and λ is 19% identical residues, where the N-terminal parts only show similarities in the DNA binding domains. In the C-terminal part, where λ carries its peptidase domain required for autocleavage, the local similarity is 21%, but the catalytic Ser and Lys residues and the G-residue of the autocleavage site are conserved. The overall similarity for the MOR anti-repressors from φ13 and TP901-1 is 65%
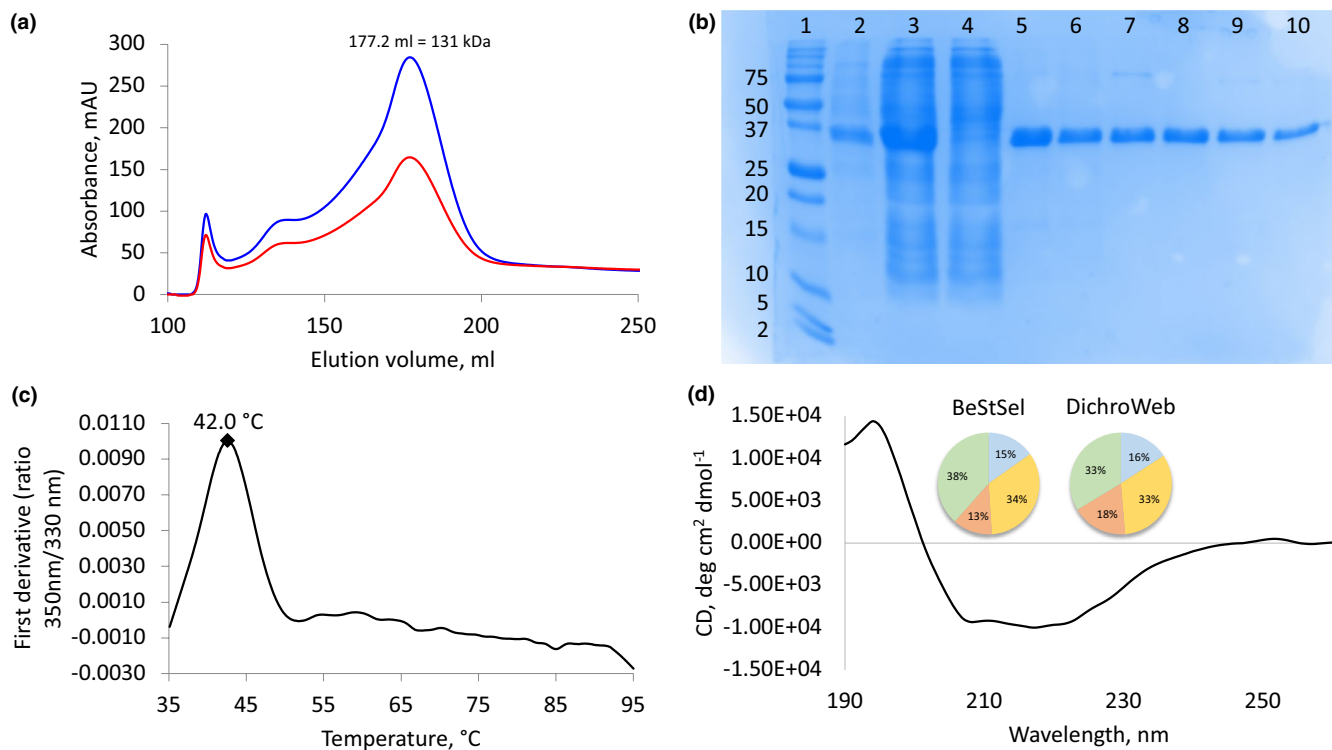
FIGURE A3 Purification and characterization of tagged φ13 rCI. (a) SEC chromatogram of φ13 rCI. The absorbance at 260 and 280 nm are shown in red and blue, respectively. The largest peak eluted at 177.2 ml corresponding to a tetramer. (b) SDS-PAGE gel showing the different steps of expression and purification of φ13 rCI. Lane 1: Precision Plus Protein™ Dual Xtra Prestained Protein Standard marker, lane 2: cell pellet diluted in water, lane 3: cell lysate after sonication and centrifugation, lane 4: HisTrap HP 1 ml flowthrough, lane 5: HisTrap HP 1 ml eluate, lane 6–10: five fractions from SEC covering the peak from 110 to 185 ml. The molecular weights of standards in kDa are shown on the left. (c) The first derivative of the ratio between 350 and 330 nm measured with DSF. The point of the inflection temperature is marked with a diamond. (d) CD spectrum of φ13 rCI with the results from the deconvolution using BeStSel and DichroWeb inserted as pie charts. The predicted secondary structure types of helix, strand, turns, and unordered are colored blue, yellow, red, and green, respectively, for both BeStSel and DichroWeb predictions

TABLE A1 A complete list of bacterial strains used in this study. Strain, species, a short description, and reference of all strains used in this study. See main text for a reference list

Strain	Species	Short description or relevant genotype	Reference or source
168	_B. subtilis_		Burkholder and Giles (1947)
8325-4	_S. aureus_	NCTC8325 phage cured	Novick (1967)
8325-4 φ13-kana	_S. aureus_	8325-4 lysogenized with φ13-kana	Tang et al. (2017)
IM08B	_E. coli_	K12 DH10B _Δdcm hsdMS_	Monk et al. (2015)
CSK8	_B. subtilis_	168 _thrC_::pCSK2 expressing the "lytic" phenotype	This study
CSK9	_B. subtilis_	168 _thrC_::pCSK2 expressing the "lysogenic" phenotype	This study
CSK10	_B. subtilis_	168/pCSK3 expressing the "lytic" phenotype	This study
CSK11	_B. subtilis_	168/pCSK3 expressing the "lysogenic" phenotype	This study
CSK19	_E. coli_	IM08B/pCSK3	This study
CSK26	_E. coli_	IM08B/pCSK9	This study
CSK32	_S. aureus_	8325-4/pCSK3 expressing the "lytic" phenotype	This study
CSK33	_S. aureus_	8325-4/pCSK3 expressing the "lysogenic" phenotype	This study
CSK44	_E. coli_	IM08B/pYL112Δ19	This study
CSK45	_S. aureus_	8325-4/pYL112Δ19	This study
CSK46	_S. aureus_	8325-4 φ13-kana/pYL112Δ19	This study
CSK47	_S. aureus_	CSK45 _geh_::pCSK9 expressing the "lytic" phenotype	This study
CSK48	_S. aureus_	CSK45 _geh_::pCSK9 expressing the "lysogenic" phenotype	This study
CSK50	_S. aureus_	8325-4 φ13-kana/pCSK3 expressing the "lysogenic" phenotype	This study
CSK51	_S. aureus_	8325-4 φ13-kana/pCSK3 expressing the "lytic" phenotype	This study
CSK52	_S. aureus_	8325-4 φ13-kana _geh_::pCSK9 expressing the "lysogenic" phenotype	This study
CSK54	_E. coli_	IM08B/pCL25	This study
CSK56	_S. aureus_	CSK46 _geh_::pCL25	This study
CSK57	_E. coli_	IM08B/pNZlac	This study
CSK59	_S. aureus_	8325-4/pNZlac	This study
CSK60	_S. aureus_	8325-4 φ13-kana/pNZlac	This study
CSK65	_E. coli_	IM08B/pCSK12	This study
CSK67	_S. aureus_	CSK46 _geh_::pCSK12 expressing the "lysogenic" phenotype	This study
CSK68	_S. aureus_	CSK45 _geh_::pCL25	This study
CSK69	_S. aureus_	CSK45 _geh_::pCSK12 expressing the "lysogenic" phenotype	This study
CSK70	_B. subtilis_	168 _thrC_::pCSK11 expressing the "lysogenic" phenotype	This study
CSK77	_E. coli_	IM08B/pCSK13 expressing the "lysogenic" phenotype	This study
CSK78	_S. aureus_	8325-4/pCSK13 expressing the "lysogenic" phenotype	This study
CSK79	_S. aureus_	8325-4 φ13-kana/pCSK13 expressing the "lysogenic" phenotype	This study
CSK80	_B. subtilis_	168/pCSK13 expressing the "lysogenic" phenotype	This study

TABLE A2 Primers used in this study

Primer name	Sequence (5' to 3')
MK740	Cy5-GTAATACGACTCACTATAGG
MK741	Cy5-CCTTTTGTGTGAAAGTTACC
MK860	AAAAGGATCCGTGATTTGTTCCATTGTGC
MK861	AAATCTAGATTAAAGCGCTAAATATACGTTATTAATCAC
MK862	AAAAGCATGCGTGATTTGTTCCATTGTGC
MK863	AAAAGAATTCTTAAAGCGCTAAATATACGTTATTAATCAC
MK867	GTAATACGACTCACTATAGGATAATAAAGCTTGTTGAACAAAAATTC
MK868	CCTTTTGTGTGAAAGTTACCACTTTACACCTTGTTTTGAATC
MK869	GTAATACGACTCACTATAGGGACTTGATTCAAAACAAGGTGTAAAG
MK870	CCTTTTGTGTGAAAGTTACCTGAGTAGTCGTAACACATAAAAGC
MK871	GTAATACGACTCACTATAGGATATACCGGTAGAGAAAATACAC
MK872	CCTTTTGTGTGAAAGTTACCGGATCCGTGATTTGTTCCATTGTG
MK902	AAAAAGATCTGCAGACATGGCCTGCCC
MK1038	GTTGAACAAAAATTCAACAAAAAAGTTGATAAATCATCAATTTTTGTATTG
MK1039	CAATACAAAAATTGATGATTTATCAACTTTTTTGTTGAATTTTTGTTCAAC
MK1040	CAAAACAAGGTGTAAAGTATAGTTAAGTTGATGATACGTCAACTTGAGAGGAG
MK1041	CTCCTCTCAAGTTGACGTATCATCAACTTAACTATACTTTACACCTTGTTTTG
MK1042	CACTTATATTTTTTTAAAGAAAAAGTTGATGTTATATCAACTTAAGGAGGGGCAC
MK1043	GTGCCCCTCCTTAAGTTGATATAACATCAACTTTTTCTTTAAAAAAATATAAGTG

Note: Name and sequence of primers used for plasmid construction and gel shift assays. All were primers designed specifically for this study.

TABLE A3 Lysogenization frequency after φ13-kana-infection of *S. aureus* 8325-4 and comparison to transformation of 8325-4 by pCKS3

lytic events (PFU ml⁻¹)	lysogenic events (CFU(Kan^R)ml⁻¹)	Lysogenization frequency (%)	MOI	Average lysogenization frequency	(p-value for mean equal to pCSK3)
2.8E+07	2.9E+06	9.4	1	4.6% ± 2.8%	0.87
1.1E+08	2.9E+06	2.6	1		
7.2E+06	3.2E+05	4.3	1		
1.5E+07	7.2E+05	4.6	1		
2.5E+07	6.2E+05	2.4	1		
1.9E+06	1.9E+05	9.1	0.1	3.5% ± 3.3%	0.47
1.2E+07	3.8E+05	3.1	0.1		
8.5E+05	2.1E+04	2.4	0.1		
5.5E+07	4.9E+04	0.1	0.1		
1.1E+07	3.2E+05	2.8	0.1		

Note: S. aureus strain 8325-4 was infected with φ13-kana at MOI at 1 and 0.1, and the frequency of lytic events (phage titer in PFU/ml, column 1) as well as the frequency of lysogenic events (CFU/ml after plating infected cells on TSB plates containing kanamycin, column 2). Column 3 shows the lysogenization frequency for all bacteria infected by φ13-kana (lysogenic events /(lytic events + lysogenic events)) for five biological replicates. Column 4 shows the MOI. Five biological replicates were included for both MOI 1 and MOI 0.1.5. Average lysogenization frequencies are shown in column 5. The p-values from two-sample *t*-tests of -average frequency from the infections at MOI of 1 and 0.1 against the frequency observed at transformation of 8325-4 by pCSK3 (4.9% ± 2.9%) are shown in column 6.

TABLE A4 Frequencies of colonies with the "lysogenic" phenotype after the introduction of *mor*-deficient φ13 switch plasmids into *S. aureus* or *B. subtilis* by transformation

S. aureus 8325-4		*S. aureus* 8325-4 φ13-kana		*B. subtilis* 168	
pCSK12[a]	pCSK13[a]	pCSK12[a]	pCSK13	pCSK11	pCSK13
100.0 ± 0 (99 colonies in total; n = 3)	100.0 ± 0 (440 colonies in total; n = 6)	100.0 ± 0 (477 colonies in total; n = 4)	100.0 ± 0 (n = 6)	100.0 ± 0 (n = 3)	100.0 ± 0 (n = 4)

Note: Switch plasmids were replicative (pCSK13) or required integration into the host (pCSK12 in *S. aureus*, pCSK11 in *B. subtilis*). pCSK11-13 are *mor*-deficient versions of pCSK2, pCSK9, and pCSK3, respectively. Recipient bacteria were naïve (*S. aureus* 8325-4 or *B. subtilis* 168) or φ13 lysogens (*S. aureus* 8325-4 φ13-kana). The number of biological replicates with more than 100 resulting colonies are stated in brackets. Frequencies of "lysogenic" transformant colonies on plates containing X-gal were calculated as the frequency between "lytic" and "lysogenic" in each transformation event and the average is shown here. Standard deviations are based on differences between each event.

[a]Indicates that <100 transformants obtained in some or all experiments. The total number of colonies is stated in brackets.